JACS
JOURNAL OF THE AMERICAN CHEMICAL SOCIETY
Article
pubs.acs.org/JACS

Catalytic Role of Multinuclear Palladium–Oxygen Intermediates in Aerobic Oxidation Followed by Hydrogen Peroxide Disproportionation

Andrew J. Ingram, Katherine L. Walker, Richard N. Zare, and Robert M. Waymouth*

Department of Chemistry, Stanford University, 333 Campus Drive, Stanford, California 94305-5080, United States

Supporting Information

ABSTRACT: Aerobic oxidation of alcohols are catalyzed by the Pd–acetate compound $[LPd(OAc)]_2(OTf)_2$ (L = neocuproine = 2,9-dimethyl-1,10-phenanthroline) to form ketones and the release of hydrogen peroxide, but the latter rapidly undergoes disproportionation. We employ a series of kinetic and isotope labeling studies made largely possible by electrospray ionization mass spectrometry to determine the role of intermediates in causing this complex chemical transformation. The data suggested that multiple catalytic paths for H_2O_2 disproportionation occur, which involve formation and consumption of multinuclear Pd species. We find that the trinuclear compound $[(LPd)_3(\mu^3\text{-}O)_2]^{2+}$, which we have identified in a previous study, is a product of dioxygen activation that is formed during aerobic oxidations of alcohols catalyzed by $[LPd(OAc)]_2(OTf)_2$. It is also a product of hydrogen peroxide activation during disproportionation reactions catalyzed by $[LPd(OAc)]_2(OTf)_2$. The results suggest that this trinuclear Pd compound is involved in one of the simultaneous mechanisms for the reduction of oxygen and/or the disproportionation of hydrogen peroxide during oxidation catalysis. Electrospray ionization mass spectrometry of hydrogen peroxide disproportionation reactions suggested the presence of other multinuclear Pd–O_2 species in solution. Theoretical calculations of these compounds yield some insight into their structure and potential chemistry.

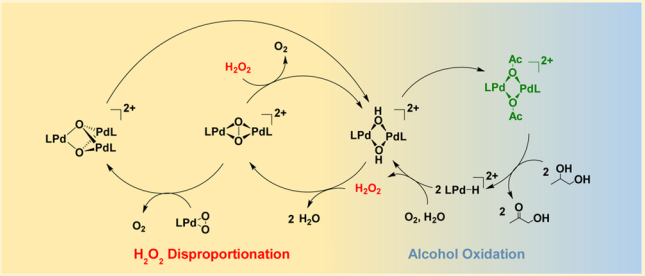

INTRODUCTION

Selective aerobic oxidation reactions constitute a broad class of important oxidative chemical transformations. Oxygen is an abundant, inexpensive, and thermodynamically potent oxidant, but is difficult to tame. It is a kinetically inert four-electron oxidant if reduced to water, but partially reduced oxygen generates peroxides and other oxidizing species that are more thermodynamically potent and often less selective than oxygen itself. Nature employs a suite of metalloenzymes with a range of mono- and multinuclear active sites for binding and activating O_2; many natural systems require coreductants, such as NADH, to absorb oxygen's excess oxidizing equivalents.[1]

Many transition metal catalysts have been devised for selective aerobic oxidations,[1−3] but in many cases our understanding of the different pathways for oxygen activation and reduction remain incomplete, limiting our ability to develop sustainable oxidation technologies.[4] Palladium catalysts are effective for a broad array of oxygen-coupled oxidation reactions[5−8] including the Wacker oxidation,[9] alcohol oxidation,[10−12] oxidative functionalization of olefins,[13,14] oxidative C–C and C–X bond-forming reactions,[15−17] and oxidative C–H functionalizations.[15,17−19] Pd complexes often function as "oxidases"[5,8] where high valent Pd (typically Pd(II)) oxidize the substrate and oxygen serves to reoxidize the resulting reduced palladium intermediates (typically Pd(0), Scheme 1).

Scheme 1. Palladium Oxidase Catalysis

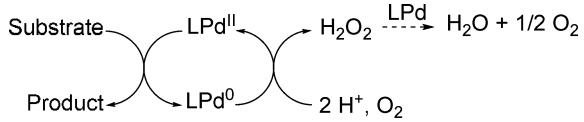

A variety of experimental and theoretical investigations have illuminated different pathways for the activation of O_2 by Pd complexes (Scheme 2) and the critical role of ligand environment on the reoxidation of reduced Pd species with O_2.[4,5,8,20,21] Significant effort has been devoted to the study of the coordination of O_2 to Pd^0,[22−29] the reactivity of Pd–H bonds with O_2,[24,30−36] and the chemistry and role of η^2-peroxido and hydroperoxy intermediates during catalysis.[26,34−37]

As oxygen is a four-electron oxidant, aerobic oxidations mediated by Pd complexes are generally proposed to generate hydrogen peroxide (H_2O_2),[5,8,38] as shown in Schemes 1 and 2. In some cases, H_2O_2 has been detected during catalytic oxidations with Pd, and when H_2O_2 is not detected, its rapid disproportionation to H_2O and O_2 has been proposed.[5,8,24,29,39] While the conversion of LPd^0 to LPd^{II} and catalytic production

Received: August 17, 2015
Published: October 7, 2015

DOI: 10.1021/jacs.5b08719
J. Am. Chem. Soc. 2015, 137, 13632−13646

Scheme 2. Mechanisms for O_2 Reduction by Reduced Pd Species[8]

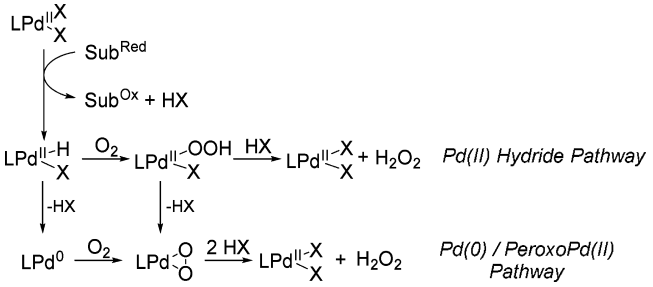

of H_2O_2 by Pd is well studied (*vide supra*), mechanistic and kinetic studies of the disproportionation of H_2O_2 by homogeneous complexes of Pd are rare,[40−43] particularly for ligand environments common to the well-studied palladium−acetate aerobic oxidation catalysts.

We have previously reported that the cationic Pd−acetate complex $[(LPd(OAc)]_2(X)_2$, **1** (L = neocuproine =2,9-dimethyl-1,10-phenanthroline, X = OTf^- or BF_4^-), is an active catalyst for the aerobic oxidation of primary and secondary alcohols, vicinal diols, polyols,[36,44−48] and carbohydrates.[49] This complex exhibits a high chemoselectivity for the oxidation of vicinal diols to hydroxyketones.[45,46,49] Air, O_2, and quinones can be used as terminal oxidants. When O_2 is used as the terminal oxidant, competitive oxidative degradation of the neocuproine ligand leads to catalyst deactivation.[36,46] Mechanistic studies revealed the formation of an inactive palladium carboxylate, **3**,[36,46] which implicated that partially reduced oxygen species, such as **4** and **5**, generated in the course of reoxidation of LPd^0 species with O_2, were responsible for competitive oxidative degradation of the neocuproine ligand (Scheme 3). This hypothesis was supported by experiments which demonstrated that the cationic acetate **1** reacts rapidly with hydrogen peroxide to generate **3**. Nevertheless, under catalytic conditions of alcohol oxidation with **1**, H_2O_2 was not detected at detection limits of less than 0.5 mM H_2O_2.[36] This suggested that either H_2O_2 is not liberated during aerobic oxidations with **1** or its disproportionation is rapid relative to catalysis. We provide evidence that the latter behavior is possible and that the disproportionation process occurs through multiple simultaneous pathways.

During the course of our investigations of these processes by electrospray ionization mass spectrometry (ESI-MS), we identified the novel trinuclear complex $[(LPd)_3(\mu^3\text{-}O)_2]^{2+}$ species, **2**.[50] An independent synthesis of **2** was devised involving the reaction of 2 equiv of the Pd peroxo complex $LPd(O_2)$, **5**, with 1 equiv of the dicationic $[LPd(MeCN)_2](BF_4)_2$, **7**, in acetonitrile at −30 °C (Scheme 4). Isotope labeling of this compound with $^{18}O_2$ revealed that it is a product of O_2-activation during catalysis, and kinetic investigations implicated that it is both chemically and kinetically competent as a catalyst precursor for the aerobic oxidation of 1,2-propanediol (propylene glycol, **PG**).[50] Mixtures of **2** and the dicationic Pd(II) complex **7** exhibited similar selectivities and rates for **PG** oxidation as that of the cationic acetate **1**.

The formation of **2** implicated a previously unrecognized multinuclear mechanism for O_2 activation by Pd. Crystallographic and theoretical analysis of **2** revealed that the oxygen atoms in **2** are fully reduced; thus the formation of **2** from 1 equiv of LPd^{II} and 2 equiv of $LPd(O_2)$ (derived from LPd^0 and O_2) represents a formal four-electron reduction of O_2 and the disproportionation of the oxidizing equivalents of two peroxide moieties. Thus, the formation of **2** represents one pathway for the complete reduction of O_2 during catalytic aerobic Pd oxidations, without the formation of partially reduced H_2O_2. Furthermore, the release of O_2 during the synthesis of **2** suggested that this process might also provide a mechanistic basis for H_2O_2 disproportionation during catalysis by Pd−acetate oxidation catalysts.

Herein, we describe a detailed mechanistic study of H_2O_2 disproportionation by the cationic Pd−acetate complex **1** and

Scheme 3. Proposed Mechanism for Alcohol Oxidation with 1

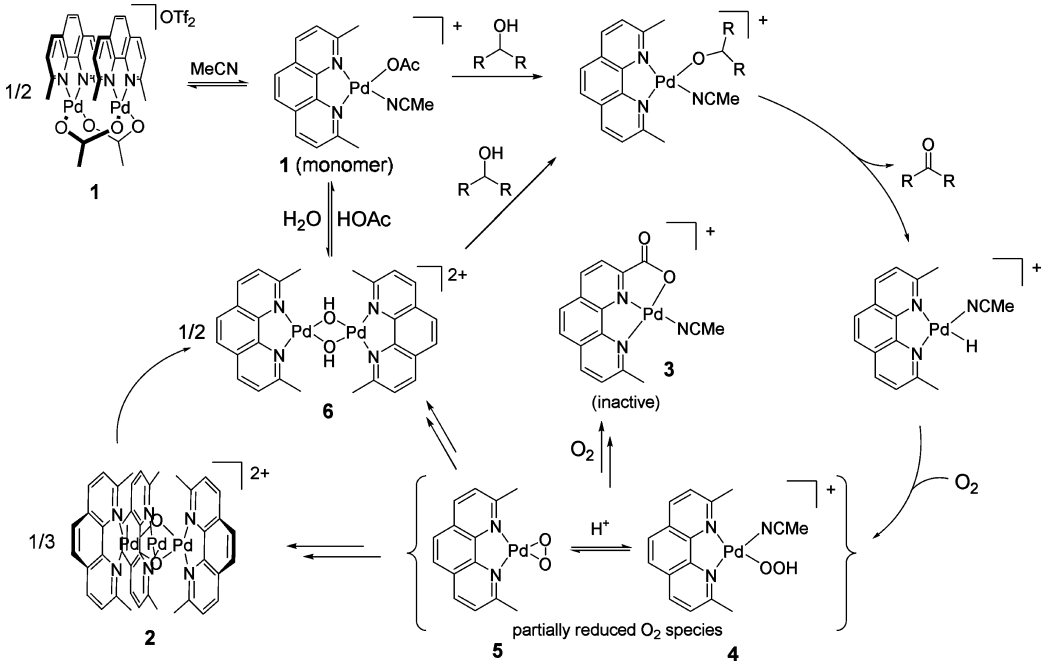

DOI: 10.1021/jacs.5b08719
J. Am. Chem. Soc. 2015, 137, 13632−13646

Scheme 4. Synthesis and Proposed Mechanism and Formation of 2

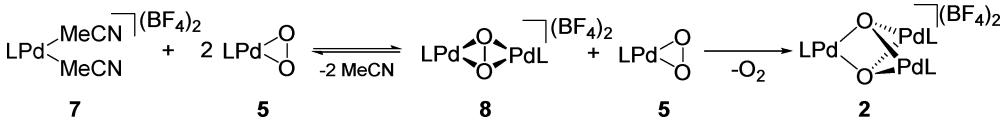

the role of H_2O_2 disproportionation reactions during the course of aerobic alcohol oxidations by **1**. These studies demonstrate that **1** and **2** are both active hydrogen peroxide disproportionation catalysts and shed light on the role of multinuclear Pd intermediates in the activation of O_2 and the catalytic disproportionation of H_2O_2. In contrast to the rich variety of multinuclear metalloenzymes and coordination compounds in biology and chemistry which reduce molecular oxygen, to date there are relatively few reports[40,50−53] of multinuclear activation of oxygen by palladium(0) species. The kinetics, reactivity, isotope labeling, ESI-MS, and NMR results highlight a complex catalytic reaction network for **1** in the reduction of O_2 to H_2O and the disproportionation of H_2O_2 into O_2 and water. The data clearly show that there are multiple catalytic paths for O_2 reduction and/or H_2O_2 disproportionation and that the trinuclear complex **2** as well as other multinuclear Pd species are both formed and consumed during the course of O_2 reduction and H_2O_2 disproportionation. We also provide evidence for the formation of novel binuclear and trinuclear Pd−O_2 intermediates during H_2O_2 disproportionation reactions with O_2; however, their role in catalysis is currently unclear. Preliminary theoretical investigations of these species yield some structural and chemical insight into the activation of O−O bonds by Pd in this system.

RESULTS AND DISCUSSION

A variety of Pd complexes bearing neocuproine ligands, bathocuproine ligands (bathocuproine = 2,9-dimethyl-4,7-diphenyl-1,10-phenanthroline, or 4,7-diphenylneocuproine), and deuterated neocuproine ligands were prepared and utilized for the present investigations (Chart 1).

Chart 1. Complexes Utilized for H_2O_2 Disproportionation/Diol Oxidation

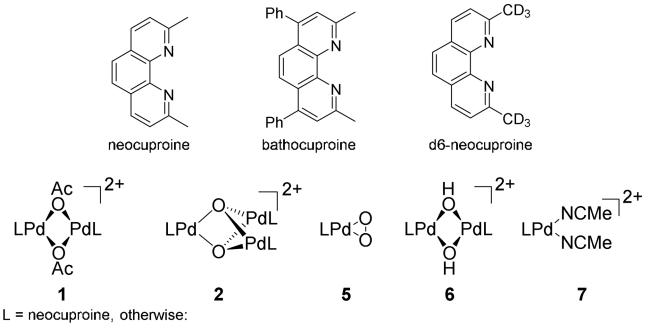

Catalytic Disproportionation of Hydrogen Peroxide by Cationic Pd Complex 1. To assess the role of H_2O_2 disproportionation in the activation of O_2[5,8] by the Pd−acetate complex **1**, we investigated the stoichiometric and catalytic reactivity of **1** with hydrogen peroxide. In the presence of 10 mol % of **1** (relative to H_2O_2), O_2 evolves over the course of approximately 45 min and then ceases, indicative of the simultaneous catalytic disproportionation of H_2O_2 and oxidative degradation of the Pd complex. ESI-MS analysis of the reaction mixtures after oxygen evolution ceased revealed ions corresponding to the previously isolated Pd carboxylate **3**, as well as ions corresponding to the partially oxidized complexes **9** and **10** which had been observed during ESI-MS of aerobic alcohol oxidations with **1** (Scheme 5).[50] These assignments were corroborated by ^{1}H NMR analysis (Figure S2).[54]

Scheme 5. H_2O_2 Disproportionation by 1

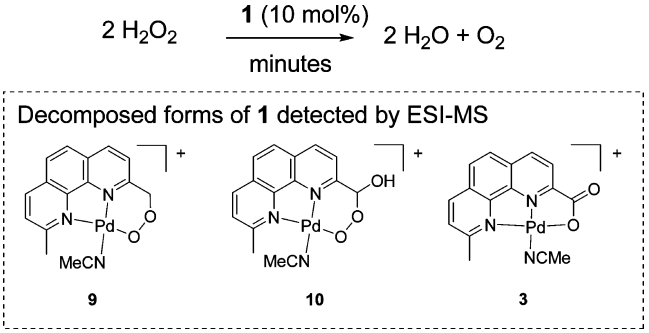

For quantitative analysis, hydrogen peroxide disproportionation experiments were carried out in a custom-designed apparatus[55] designed to manometrically monitor the generation of O_2 gas with time. To assess the mass balance for the H_2O_2 disproportionation reactions, a sealed vessel was charged with 1.0 mL of 100 mM H_2O_2 (100 μmol H_2O_2), 5 mM **1** ([Pd] = 10 mM, 10 μmol, 10%), and 10 mM HOAc in 9:1 MeCN/H_2O, and the increase in pressure arising from $O_{2(g)}$ production was monitored. After gas evolution ceased (approximately 45 min), $KMnO_4$ titration of the residual H_2O_2 indicated that 74 μmols of the H_2O_2 had been consumed, corresponding to 7.4 turnovers (mmol H_2O_2/mmol Pd) of **1**. The pressure increase in the reaction vessel corresponded to the production of 25 μmol $O_{2(g)}$, (i.e., 50 μmol of H_2O_2 were converted to $O_{2(g)}$ out of the 74 μmol consumed). The remainder of the consumed H_2O_2 (24 μmol) can be accounted for by the oxidizing equivalents necessary to decompose **1** to a mixture of **3**, **9**, and **10**. An independent reaction was carried out in in 9:1 d_3-MeCN/H_2O, and a ^{1}H NMR spectrum of the reaction mixture was recorded after 45 min. ^{1}H NMR revealed a mixture predominantly containing the oxidized Pd species **3** (approximately 1.3 μmol), **9** (approximately 6.1 μmol), and **10** (approximately 1 μmol), along with a small concentration of the trinuclear species **2** (approximately 0.5 μmol). The oxidation of **1** to this mixture of **3**, **9**, and **10**[56] was calculated to consume approximately 20 μmol of H_2O_2, accounting for 94 ± 4% of the consumed H_2O_2 (Table S1). This experiment indicates that, under conditions where oxidative degradation of **1** is insignificant, monitoring $O_{2(g)}$ is a good metric for the consumption of H_2O_2 by the disproportionation process.

Kinetic studies for the disproportionation of H_2O_2 were carried out by measuring the initial rates of O_2 generation, prior

DOI: 10.1021/jacs.5b08719
J. Am. Chem. Soc. 2015, 137, 13632−13646

to significant oxidative degradation of **1**.[57] Initial rates were determined approximately 1 min after initiation and during the time the pressure increase was still linear with time (i.e., at low H_2O_2 conversion and before noticeable degradation of **1**). At high [**1**] or low [H_2O_2], decomposition of **1** was too fast for our system to measure an accurate initial rate. Stock solutions of **1** were made in 0.1 M HOAc to ensure stability,[58] and reactions were performed in 9:1 MeCN/H_2O solvent such that the production of H_2O did not appreciably change the concentration of H_2O. Figure 1 shows the results of these experiments.

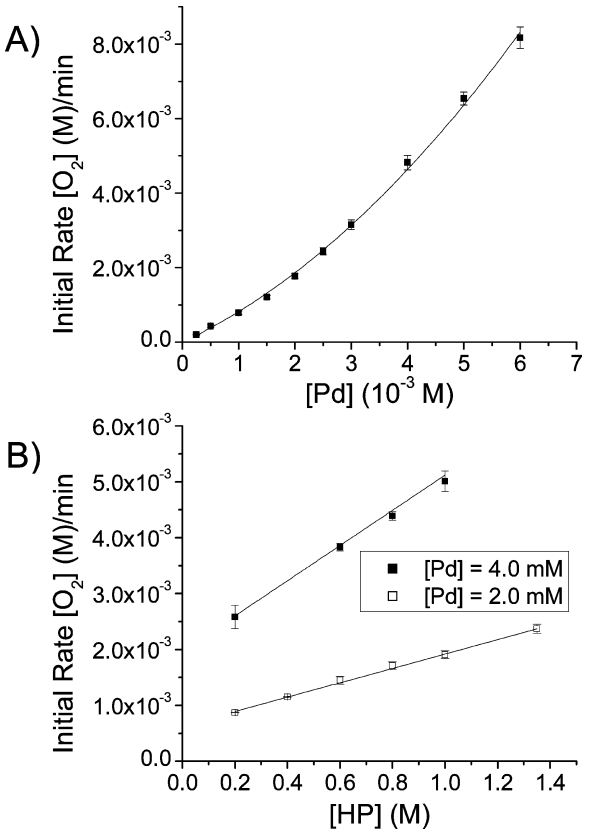

Figure 1. Initial rates for the disproportionation of H_2O_2 (**HP**) by **1** with 10 mM HOAc in 1:9 H_2O/MeCN. (A) Initial rate dependence on [Pd] from 0.25−6.0 mM at $[H_2O_2]_i$ = 1.0 M, where [Pd] is the total [Pd] (i.e., double the [**1**]). Fit corresponds to eq 1. (B) Initial rate dependence on [H_2O_2] from 0.2−1.35 M at [Pd] = 2.0 mM (□) and 4.0 mM (■). Fits correspond to eq 1. All reactions performed at least in duplicate. Most reactions performed in triplicate or more. 6% or experimental ±1σ error bars (whichever was greater) are shown.

The data in Figure 1 reveal that the initial rates of O_2 evolution exhibit a complex dependence on both the initial concentration of Pd and H_2O_2. Analysis of the initial rates as a function of the concentrations of Pd, H_2O_2, HOAc, and H_2O yielded the rate law (eq 1):

$$\frac{d[O_2]}{dt} = k_1[H_2O][HOAc][Pd]^2 + k_2[H_2O_2][Pd] \quad (1)$$

where $k_1 = (2.05 \pm 0.22) \times 10^3$ M^{-3} min^{-1} and $k_2 = (7.03 \pm 0.29) \times 10^{-1}$ M^{-1} min^{-1} (see Supporting Information for derivation and comparison with other unsuccessful models used to fit the data). The mixed-order rate law (eq 1) is suggestive of several competitive pathways for H_2O_2 disproportionation that exhibit a complex dependence on the concentrations of Pd, H_2O_2, HOAc, and H_2O.

To assess the possible contribution of a radical chain process for the H_2O_2 disproportionation reactions catalyzed by **1**, the rate of H_2O_2 disproportionation was investigated in the presence of radical scavenging 2,6-diisopropylphenol (**DiPP**) and butylated hydroxytoluene (**BHT**). Low concentrations (<50 mM) of **DiPP** or **BHT** suppressed the rate of O_2 evolution. This effect saturates between 0.1 and 0.2 M for **DiPP** and approaches saturation at 0.1 M for **BHT**, which is the solubility limit for **BHT** in 1:9 H_2O/MeCN (Figures S4 and S5). When the system is saturated in **DiPP** (0.2 M) or **BHT** (0.1 M), the rate of H_2O_2 disproportionation decreases approximately 2-fold.[59]

To determine whether **1** is catalyzing the oxidation of **DiPP** by H_2O_2, 0.2 M H_2O_2 was treated with 7 mM **1** in the presence of 0.1 M **DiPP** (14% Pd loading relative to **DiPP**). Significant gas evolution was observed, and at the end of the reaction ^{1}H NMR showed that 93% of the H_2O_2 and 44% of the **DiPP** had been consumed. This corresponded to the consumption of approximately 3.4 **DiPP** per Pd, which indicated that the consumption of **DiPP** was catalytic in Pd. GC-MS of similar reaction mixtures suggested that the major product of **DiPP** oxidation was the radical coupling product, 4,4′-bis(2,6-diisopropylphenol).[60] The inhibition of the rate of O_2 evolution with phenols is consistent with either suppression of a radical chain mechanism or a competitive phenol oxidation that inhibits the Pd-mediated process for the H_2O_2 disproportionation reaction.

To further evaluate the possibility of a radical chain mechanism, the influence of the Pd concentration on the initial rates of O_2 evolution was measured in the presence of high concentrations of **DiPP** (0.2 M) or **BHT** (0.1 M, the solubility limit). The initial rates of O_2 evolution in the presence of 0.1 M **BHT** (the saturation limit) or 0.2 M **DiPP** in 9:1 MeCN/H_2O are slower but conform to a partial rate law that is very similar to that observed in the absence of the phenols (Table S5 and Figures S4 and S5). These data argue against a radical chain mechanism for H_2O_2 disproportionation, as the order of the rate law would be expected to change in the presence of radical chain breaking agents such as phenols.[61] The observed catalytic consumption of **DiPP** and the differences in rates observed in the presence of **DiPP** or **BHT** imply that catalytic phenol oxidation is a competitive process with H_2O_2 disproportionation.

Electrospray Ionization Mass Spectrometry Studies of Hydrogen Peroxide Disproportionation. To interrogate reactive intermediates generated during the catalytic disproportionation of H_2O_2 by **1**, the reactions were monitored continuously by ESI-MS utilizing a method described previously.[62−64] A solution containing 1.0 M H_2O_2 and 0.5 mM **1** with 9:1 MeCN/H_2O solvent was monitored in both the presence and absence of 10 mM HOAc. Prominent and significant Pd containing ions are shown in Scheme 6. To emphasize the difference between gas-phase compounds and solution-phase compounds, the detected gas-phase ions are named as A^{X+} (i.e., **6** is in solution, but $\mathbf{6}^{2+}$ is in the gas phase).

To assess the origin of these ions, a series of isotope labeling experiments were carried out and monitored by both ESI-MS and ^{1}H NMR (see Table 1 and the Supporting Information). For the ^{18}O-labeling experiments, an Orbitrap Fusion Tribrid Mass Spectrometer with a resolving power of at least 400 000 ($m/\Delta m$)[65] was required in order to resolve the various Pd−O

DOI: 10.1021/jacs.5b08719
J. Am. Chem. Soc. 2015, 137, 13632−13646

Scheme 6. Proposed Structures and Theoretical *m/z* of Representative Ions Detected by ESI-MS during H_2O_2 Disproportionation by 1

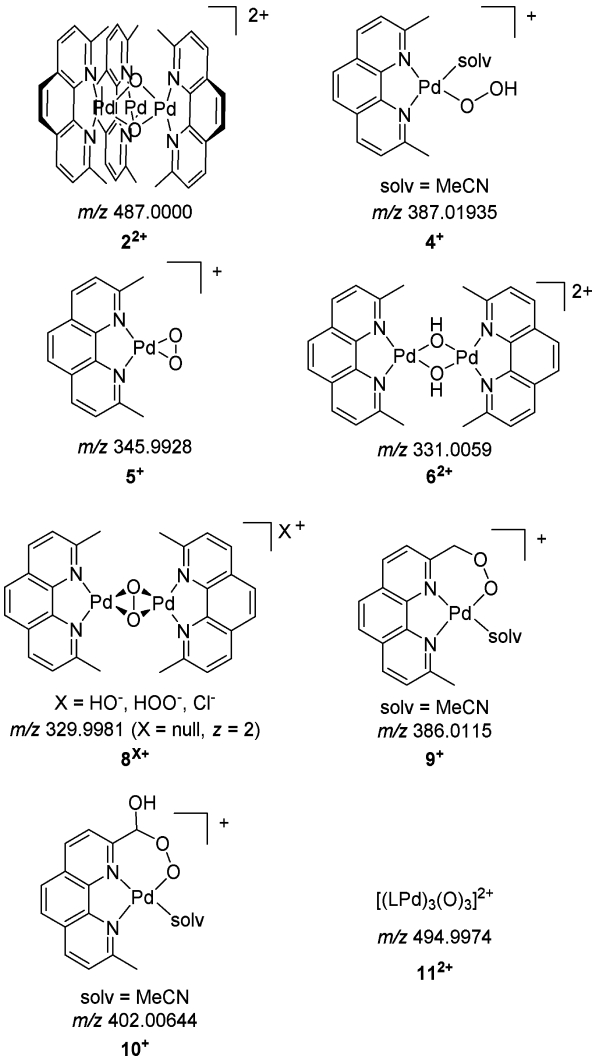

isotopologues generated. Deuterium isotope labeling experiments with the d_6-neocuproine ligand L^D (L^D = the d6-analog of neocuproine, L^H, where the $-CH_3$ groups have been replaced with $-CD_3$ groups, Chart 1) did not have such strict requirements and were carried out with an LTQ-Orbitrap Hybrid Mass Spectrometer, which can operate up to resolving powers of 100 000 at *m/z* 400.[66]

Analysis of the ESI-MS and ^1H NMR data of a H_2O_2 disproportionation reaction under standard conditions revealed that the Pd–acetate complex **1** is consumed rapidly, as the major ion observed in the ESI-MS corresponded to the bridging hydroxide complex **6**, detected as $\mathbf{6}^{2+}$ in the mass spectra as an envelope of peaks centered about *m/z* 331.0005 (reported *m/z* are for ^{106}Pd isotopologues). Ions corresponding to the Pd–acetate **1** are only present in trace amounts during H_2O_2 disproportionation in 10 mM HOAc and 1:9 H_2O/MeCN solvent. We had previously established that **6** can be prepared from the reaction of **1** with H_2O in MeCN;[36] it would appear that the generation of **6** from **1** is more efficient in the presence of H_2O_2. When a solution of the Pd–acetate **1** was treated with $H_2{}^{18}O_2$ in 1:9 $H_2{}^{16}O$/MeCN, analysis of the resulting mixture by ESI-MS revealed doubly charged ions centered at *m/z* 333.0095 (*z* = 2), corresponding to the doubly ^{18}O-labeled compound $\mathbf{6}^{2+}$ (see Table 1). This indicates that the oxygen atoms of **6** are derived from H_2O_2 and that **6** is a direct product of H_2O_2 activation during disproportionation reactions.

To test whether both oxygens from $H_2{}^{18}O_2$ are incorporated into **6** in a pairwise manner, a solution of **1** was treated with an approximately 0.9:1 mixture of $H_2{}^{18}O_2$ and $H_2{}^{16}O_2$ in 1:9 $H_2{}^{16}O$/MeCN.[67] When **1** was used to disproportionate the mixture of $H_2{}^{18}O_2$ and $H_2{}^{16}O_2$ in 1:9 $H_2{}^{16}O$/MeCN, only two distributions of ions corresponding to $\mathbf{6}^{2+}$ were observed, corresponding to the $^{16}O_2$ and $^{18}O_2$ labeled compounds and not their $^{16}O^{18}O$ isotopologues (see Table 1). This result indicates that both oxygens from H_2O_2 are incorporated pairwise into the μ-hydroxide **6**. Moreover, this crossover experiment implies that, in the presence of H_2O_2, **6** does not exchange rapidly with $H_2{}^{16}O$ on the time scale of the analysis. This phenomenon was unexpected, but implies that, during the course of H_2O_2 disproportionation, **6** is consumed faster than it equilibrates with the $H_2{}^{16}O$ solvent.

Ions corresponding to the trinuclear species, $\mathbf{2}^{2+}$ (*m/z* = 487.0003), are also detected during H_2O_2 disproportionation by **1**. ESI-MS monitoring of the mixture of 0.18 M $H_2{}^{18}O_2$ and 50 μM **1** in 1:9 $H_2{}^{16}O$/MeCN solvent revealed doubly charged ions at *m/z* 489.0042 (*z* = 2), corresponding to $\mathbf{2}^{2+}$ where both oxygen atoms of $\mathbf{2}^{2+}$ are derived from $H_2{}^{18}O_2$. These data indicate that $\mathbf{2}^{2+}$ is a product of H_2O_2 activation during catalysis (see Table 1). Furthermore, the crossover experiment where a mixture of 0.9:1 $H_2{}^{18}O_2$ and $H_2{}^{16}O_2$ in 1:9 $H_2{}^{16}O$:MeCN was disproportionated by **1** yielded only two distributions of peaks for $\mathbf{2}^{2+}$, centered about *m/z* 487.0003 and *m/z* 489.0043, respectively (see Table 1). This finding illustrated that both oxygen atoms in $\mathbf{2}^{2+}$ were derived from the same molecule of

Table 1. Relative Isotopic Abundance for Selected Species During H_2O_2 Disproportionation with 1

compound	$\mathbf{2}^{2+}$			$\mathbf{6}^{2+}$ [d]			$\mathbf{8}^{2+}$		
H_2O_2 source	$H_2{}^{16}O_2$ [a]	$H_2{}^{18}O_2$ [b]	$H_2{}^{16}O_2/H_2{}^{18}O_2$ [c]	$H_2{}^{16}O_2$	$H_2{}^{18}O_2$	$H_2{}^{16}O_2/H_2{}^{18}O_2$	$H_2{}^{16}O_2$ [d]	$H_2{}^{18}O_2$ [e]	$H_2{}^{16}O_2/H_2{}^{18}O_2$ [e]
$^{16}O_2$	100%	0%	74%	100%	8%	73%	100%	2%	64%
$^{16}O^{18}O$	0%	0%	–	0%	8%	0%	0%	0%	0%
$^{18}O_2$	0%	100%	26%	0%	84%	27%	0%	98%	36%

[a]Some isobaric peaks coalesced. Noncoalesced peaks fit as a linear sum of simulated peaks. [b]Peaks coalesced at 450 000 resolution, so the total intensities of the overlapping peaks at 100 000 resolution were fit as a linear sum of the simulated spectra for each *m/z*. [c]Peaks were partially coalesced. There was no visible evidence for an $^{16}O^{18}O$ compound, so it was excluded from the fit. Including an $^{16}O^{18}O$ compound does not improve the fit. [d]Determined by fitting all peaks to a linear sum of simulated peaks. [e]Some peaks overlapping, determined by fitting half-integer peaks which were generally well resolved.

DOI: 10.1021/jacs.5b08719
J. Am. Chem. Soc. 2015, 137, 13632–13646

H_2O_2, consistent with its involvement in H_2O_2 disproportionation (see Table 1).

During the ESI-MS monitoring experiments, an additional set of ions centered about m/z 329.9974 were also detected in relatively low abundance. These ions correspond to the molecular formula $[(LPd)_2(O_2)]^{2+}$, detected as the ion $\mathbf{8}^{2+}$. As illustrated in Scheme 4, complex **8** was previously proposed as a reactive intermediate in the formation of the trinuclear complex **2**, but had not been previously observed. Isotope labeling experiments performed with $H_2{}^{18}O_2$ and $H_2{}^{18}O_2/H_2{}^{16}O_2$ in 1:9 $H_2{}^{16}O$/MeCN solvent confirm that both oxygen atoms in the ion $\mathbf{8}^{2+}$ are derived from a single molecule of H_2O_2 (see Table 1). The ESI-MS data do not give information as to whether there is an O−O bond in $\mathbf{8}^{2+}$ (i.e., whether $\mathbf{8}^{2+}$ has a μ-peroxo or bis(μ-oxo) core). The observation of the ion $\mathbf{8}^{2+}$ under these conditions is consistent with its involvement in the formation of **2** during H_2O_2 disproportionation. Ions corresponding to various anion adducts of $\mathbf{8}^{2+}$, $\mathbf{8}^{X+}$ are also detected for X = HO^-, Cl^-, and HO_2^- (Scheme 6); however, the structure of these adducts is not clear.

An additional set of ions were detected at m/z 494.9965 during the reaction between H_2O_2 and **1**. This ion is formulated as the trinuclear Pd_3O_3 species, $\mathbf{11}^{2+}$, with a molecular formula corresponding to $[(LPd)_3(O)_3]^{2+}$, consisting of three LPd units and three oxygen atoms (Scheme 7). The reaction with H_2O_2 and **1**-L^D yielded ions centered about m/z 504.0549, indicating that this species contains 18 deuterium atoms. The reaction with $H_2{}^{18}O_2$ in 1:9 $H_2{}^{16}O$/MeCN solvent yielded a complicated set of overlapping peaks centered about nominal m/z 496. Fitting these peaks to linear sums of simulated spectra indicated that 82% of the detected $\mathbf{11}^{2+}$ was $Pd_3{}^{18}O_3{}^{2+}$ and 18% was $Pd_3{}^{18}O_2{}^{16}O^{2+}$, similar to the distribution of the ^{18}O label in $\mathbf{6}^{2+}$ (no $Pd_3{}^{16}O_3{}^{2+}$ or $Pd_3{}^{18}O^{16}O_2{}^{2+}$ was detected; see Supporting Information). In the experiment where a mixture of $H_2{}^{18}O_2/H_2{}^{16}O_2$ was reacted with **1** in 1:9 $H_2{}^{16}O$/MeCN, all four possible isotopologues were detected. The relative abundance of each isotopologue indicated that one oxygen atom is derived from **6**, whereas the other two are derived from H_2O_2. In other words, $\mathbf{11}^{2+}$ appears to be a combination of **6** and the hydroperoxide **4** (Scheme 6). The structure of the $Pd_3O_3{}^{2+}$ core of $\mathbf{11}^{2+}$ is not clear from the current data; some plausible structures are shown in Scheme 7. At this point, the data do not indicate whether $\mathbf{11}^{2+}$ plays a specific role in catalysis, but similar Mn_3O_3 species have been proposed as intermediates of H_2O_2 disproportionation with Mn catalysts.[68]

In order to gain insight on the speciation of Pd over the course of a H_2O_2 disproportionation reaction, a solution of 1.0 M H_2O_2 in 1:9 H_2O/MeCN with 10 mM HOAc was injected with a sample of **1** ([**1**] = 0.5 mM) and monitored continuously by ESI-MS.[50,63,69] The data for this experiment are shown in Figure 2A. Production of O_2 was monitored in an independent, simultaneous experiment, and the measured rate of reaction vs time is shown in Figure 2B. While precise concentrations are very difficult to obtain from ESI-MS of complicated mixtures, some qualitative insight can be gleaned from Figure 2. At the end of the reaction, the predominant ions observed are those corresponding to the oxidized complexes $\mathbf{9}^+$ and $\mathbf{10}^+$, consistent with their role as inactive, oxidized forms of **1**. Ions corresponding to the trinuclear complex $[(LPd)_3(O)_3]^{2+}$ $\mathbf{11}^{2+}$ are only present in the earliest stages of the reaction, and the relative abundance of these ions correlates with those corresponding to the μ-hydroxide $\mathbf{6}^{2+}$, which is the most abundant species during the initial phase of the reaction. The abundance of $\mathbf{6}^{2+}$ in the ESI-MS correlates reasonably well with the initial rate of O_2 production vs time; however, the signal for $\mathbf{6}^{2+}$ decays faster than the rate of O_2 production after approximately 10 min (see Figure S15 for an overlay of these curves). Ions corresponding to the trinuclear complex $\mathbf{2}^{2+}$ increase in relative abundance over the course of the reaction, reach a maximum after 10 min, and then slowly decay away as the reaction progresses. Combined with the isotope labeling data, this behavior indicates that both **6** and **2** are generated and consumed in the course of H_2O_2 disproportionation and thus may represent different Pd-containing reactive intermediates during catalysis with H_2O_2.

Disproportionation of H_2O_2 with 2 and 7. The observation of **2** during ESI-MS and NMR monitoring of

Scheme 7. Possible Structures for $\mathbf{11}^{2+}$

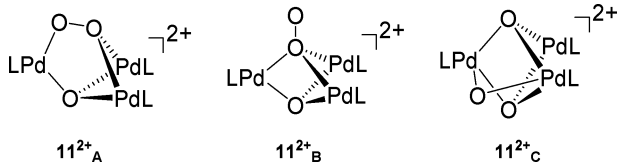

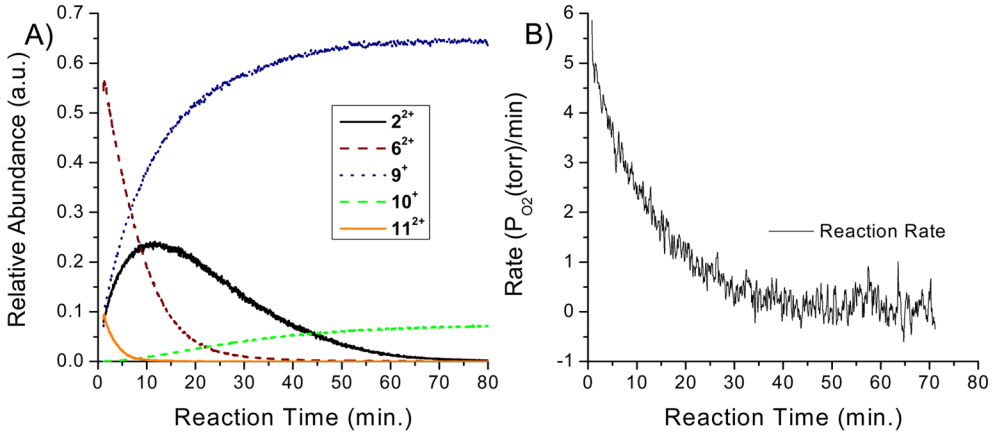

Figure 2. Online ESI-MS Monitoring of H_2O_2 disproportionation with **1**. (A) Relative abundance of significant Pd-containing species. Normalized to the total intensity. (B) Instantaneous rate of O_2 production as reaction progresses. Conditions: [H_2O_2] = 1.0 M, [**1**] = 0.5 mM, in 10 mM HOAc in 1:9 H_2O/MeCN.

DOI: 10.1021/jacs.5b08719
J. Am. Chem. Soc. 2015, 137, 13632−13646

Scheme 8. Observed Reactivity of 2

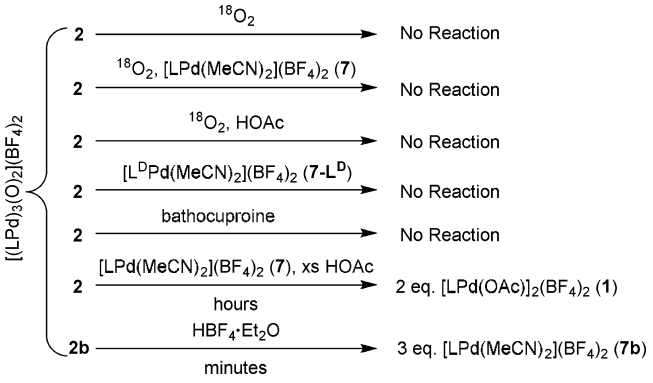

mixtures of H_2O_2 and **1** prompted us to study the activity of the trinuclear complex **2** as well as the dication **7** as precatalysts for H_2O_2 disproportionation. The Pd(II) dication **7** is an active catalyst for the disproportionation of H_2O_2 with nearly identical rates and activities as that of **1** at 0.5 mM [Pd] and 1.0 M H_2O_2 (Figure S16, Table S8). The trinuclear complex **2** is also an active hydrogen peroxide disproportion catalyst, but its activity is lower than that of both **1** and **7** on a per Pd basis. Addition of HOAc or **7** to reactions with **2** increased the rate of H_2O_2 disproportionation, but even in these cases, the activity of **2** is lower than that of **1** (see Supporting Information, Figure S16, Table S8). This behavior is in contrast to the activity of **2** and **7** in the oxidation of alcohols,[50] where mixtures of **2** and **7** had identical reactivity as **1** in the oxidation of 1,2-propanediol.

Reactivity of $Pd_3O_2^{2+}$ Complex 2. The observation that the trinuclear complex **2** is generated during the course of hydrogen peroxide disproportionation and is itself an active disproportionation catalyst prompted us to investigate its reactivity in more detail. In particular, we investigated the ligand exchange dynamics of **2** under a variety of conditions. The oxygen ligands of **2** do not readily exchange with gaseous O_2: when MeCN solutions of **2** (0.1 mM) in a sealed flask were exposed to gaseous $^{18}O_2$ (approximately 120 Torr $^{18}O_2$ in N_2), no incorporation of ^{18}O into **2** was observed over the course of 4 h. Addition of 17 equiv of HOAc or 1 equiv of $[LPd(CH_3CN)_2]^{2+}$ **7** to similar solutions of **2** also did not result in measurable incorporation of ^{18}O. These experiments illustrate that, in the absence of a reducing agent, **2** does not exchange its oxygen ligands with gaseous O_2.

To assess if **2** is in reversible equilibrium with its precursors, **5** and **7** (Scheme 4), the isotopically labeled complex, 7-L^D, was prepared from d6-neocuproine (L^D), a deuteriated version of neocuproine (L^H). Mixtures of **2** (0.1−1 mM) and 7-L^D (0.1−1 mM) in MeCN showed no incorporation of L^D into **2** or incorporation of L^H in 7-L^D by ESI-MS or ^1H NMR over the time scale of hours. In fact, samples of **2** in the presence of 7-L^D decomposed within 16 h into unknown precipitates without any observable exchange with 7-L^D. Samples of **2** also did not exchange with the free ligand, bathocuproine. These studies conclusively showed that **2** does not exchange with or establish a reversible equilibrium with its constituent reagents, **5** and **7**. These results are summarized in Scheme 8.

The experiments above indicate that, once formed, the trinuclear complex **2** does not exchange readily with O_2, the ligand bathocuproine, or $[LPd(CH_3CN)_2]^{2+}$ (**7**). An additional isotope scrambling experiment was carried out to test for the reversible formation of reactive intermediates during the formation of **2**. This experiment involved treatment of an excess of the labeled Pd^{II} cation 7-L^D (4.7 equiv) to a limiting amount of the perprotio Pd peroxo **5** (1 equiv), at room temperature in MeCN to generate **2** (Scheme 9). ^1H NMR and ESI-MS of the resulting solution indicated that the labeled ligand L^D was statistically distributed between **2** and the residual dication **7** (see Table S9 and Figure S17). Because **2** did not react or undergo ligand exchange with the dication **7**, this experiment provided evidence for the rapid and reversible formation of an intermediate that readily scrambles the LPd unit. No ligand substitution was observed within minutes at room temperature in a mixture of **5b** and neocuproine. The formation of **2** was fast and occurred in under a minute at room temperature. Therefore, direct exchange of L^D for L^H in **5** is not a reasonable explanation for the observed scrambling process.[70] A possible candidate for this intermediate is a dinuclear dicationic Pd bridging peroxo complex **8**, which we had previously proposed[50] as an intermediate in the formation of **2** and which others had proposed as an intermediate in hydrogen peroxide disproportionation.[40] While the precise structure of the cationic dinuclear peroxo complex **8** is not clear, the fact that the ion 8^{2+} is observed by ESI-MS in the course of H_2O_2 disproportionation experiments is consistent with its role as a reactive intermediate in H_2O_2 disproportionation and in the formation of **2**. Furthermore, because both oxygen atoms of the ions 2^{2+} and 8^{2+} are ^{18}O-labeled in ESI-MS of solutions with $H_2{}^{18}O_2$ and $H_2{}^{16}O_2$, this exchange process is likely a pairwise transfer of oxygen atoms, such as the reversible exchange of a peroxo, O_2^{2-}, ligand.

Conversion of Trinuclear Species to Pd−Acetate. The observation that the trinuclear complex **2** is generated and consumed in the course of H_2O_2 disproportionation with the Pd−acetate catalyst precursor **1** prompted us to investigate the conditions under which complex **1** could be regenerated from **2**. Treatment of an equimolar mixture of **2** and the dicationic $[LPd(CH_3CN)_2]^{2+}$ **7** with 4 equiv of HOAc (relative to total Pd) in MeCN yielded the palladium acetate **1** quantitatively after 24 h. To investigate the kinetics of this process, we prepared the analogous bathocuproine complexes[26] **1b**, **2b**, **5b**, and **7b** (bathocuproine = 2,9-dimethyl-4,7-diphenyl-1,10-phenanthroline or 4,7-diphenylneocuproine), as these complexes are more soluble than the neocuproine analogs. Control experiments show that the bathocuproine complexes exhibit similar chemistry to the neocuproine complexes.

Scheme 9. Proposed Mechanism for Isotope Scrambling during Formation of 2

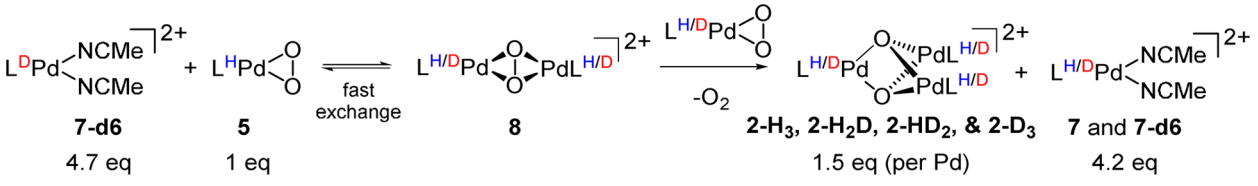

DOI: 10.1021/jacs.5b08719
J. Am. Chem. Soc. 2015, 137, 13632−13646

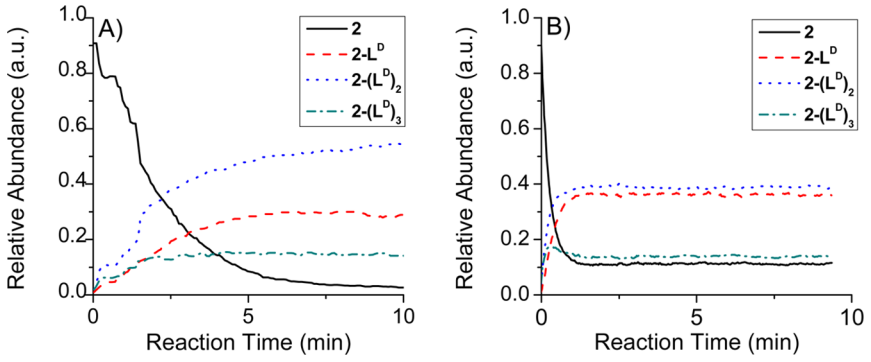

Figure 3. Measured (A) and simulated (B) isotope incorporation into **2** during H_2O_2 disproportionation. (A) Relative abundance of **2**, **2**-L^D, **2**-$(L^D)_2$, and **2**-$(L^D)_3$ observed by ESI-MS as a function of time. Conditions: [**2**] = 0.11 mM; [**7**-L^D] + [**7**] = 0.64 mM, **7**-L^D:**7** = 3.8; [H_2O_2] = 0.5 M in 1:9 H_2O/MeCN. (B) Stochastic simulation of the relative abundance of **2**, **2**-L^D, **2**-$(L^D)_2$, and **2**-$(L^D)_3$ as a function of time.

Scheme 10. Proposed Mechanism for Incorporation of L^D into 2 during H_2O_2 Disproportionation

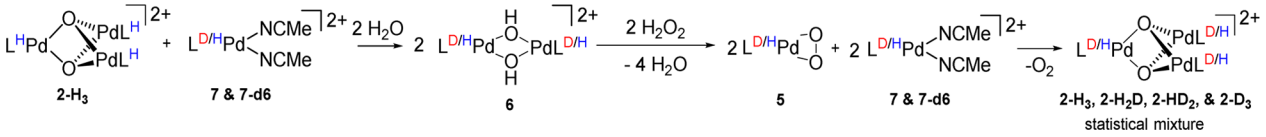

The kinetics for the conversion of the trinuclear complex **2b** to the cationic Pd–acetate **1b** was studied by ^{1}H NMR under pseudo-first-order conditions with [**2b**] = 1 mM, excess **7b** (8–20 mM), and excess HOAc (37–62 mM). The decrease in [**2b**] corresponded to the rate law shown in eq 2 (see Supporting Information for details). This process was found to be first-order in each reagent with the third-order rate constant, k_{1b} = 17.6 ± 2.8 M^{-2} min^{-1}. No reaction is observed without added HOAc, and without **7b** the rate of decay of **2b** is much slower and the reaction does not quantitatively form **1b**. We propose that conversion of **2b** to **1b** is initiated by protonation of an oxygen atom of **2b** and that the role of **7b** in this reaction is to coordinate to HOAc to increase its acidity. To test if strong acids react more rapidly with **2b**, 50 equiv of HOAc were added to a 0.8 mM solution of **2b**. The reaction was monitored for 24 h, after which 62% of **2b** remained (in the presence of 10 mM **7b** at the same [HOAc], the $t_{1/2}$ of **2b** is approximately 1 h). Adding one drop of a strong acid, HBF_4·Et_2O, to this solution converted the remaining **2b** to **7b** within 5 min.

$$-\frac{d[\mathbf{2b}]}{dt} = k_{1b}[\mathbf{2b}][\mathbf{7b}][\mathrm{HOAc}] \quad (2)$$

The rate of conversion of **2b** to **1b** in the presence of **7b** and HOAc is slower than the rate of hydrogen peroxide disproportionation or alcohol oxidation by the neocuproine Pd–acetate catalyst precursor **1**. For H_2O_2 disproportionation with 0.2 M H_2O_2 (for [Pd] from 1.25–7.5 mM) the rough turnover frequency (TOF per Pd) varies from 0.57 to 2.00 min^{-1}, whereas the pseudo-first-order rate constant for the conversion of **2b** to **1b** with 2.5 mM Pd ([**2b**] = 0.84 mM) is 3.54 × 10^{-4} min^{-1}. For alcohol oxidation of **PG** with 2.5 mM Pd from **1**, the TOF per Pd is between 0.09 and 0.33 min^{-1}, 3 orders of magnitude faster than the rate of the conversion of **2b** to **1b** (Table S12). However, under protic conditions (10% water, 10 mM HOAc) the conversion of **2b** to **1b** with 4.5 mM Pd (**2b**:**7b** = 1:0.5) increases to 3.51 × 10^{-2} min^{-1} (0.11 min^{-1} per Pd) and approaches that of alcohol oxidation on a per Pd basis. Thus, while the trinuclear complex **2** is a chemically competent precursor for hydrogen peroxide disproportionation and alcohol oxidation, its reactivity is highly dependent on conditions and the rate of conversion of **2b** to **1b** is sufficiently slow that pathways involving **2** as a reactive intermediate cannot be the predominant or sole pathway for hydrogen peroxide disproportionation (see the following discussion and Supporting Information for more details and a proposed mechanism).

Role of 2 during Catalysis with 1: Hydrogen Peroxide Disproportionation. The formation of **2** during both H_2O_2 disproportionation and alcohol oxidation suggested that it is an important intermediate in the speciation of Pd during these processes. Its relatively slow reactivity and dynamics provided a unique opportunity to investigate its formation and role during catalysis. We designed an isotope incorporation experiment to provide further insight into the role of **2** during hydrogen peroxide disproportionation and alcohol oxidation.

An isotope scrambling experiment was devised to assess the rate at which the trinuclear complex **2** is consumed and reformed relative to the rate at which hydrogen peroxide is disproportionated. Using H_2O_2 as the substrate, a cocatalytic mixture of unlabeled **2** with a combination of **7** and **7**-L^D (**2** = 0.11 mM, [**7**] + [**7**-L^D] = 0.64 mM, **7**-L^D:**7** = 3.8) was used to disproportionate 0.5 M H_2O_2 in 1:9 H_2O/MeCN. O_2 production and online ESI-MS data were gathered from two simultaneous, parallel reactions. The resulting speciation of the different isotopologues of **2** as a function of reaction time is displayed in Figure 3A. As is evident from Figure 3A, the labeled ligand L^D is incorporated into **2** during the course of the hydrogen peroxide disproportionation; these data clearly indicate that the trinuclear complex **2** is consumed and reformed during the catalytic reaction.

Shown in Figure 3B is the predicted speciation of isotopologues of **2** as a function of time under the assumption that one turnover of **2** would involve the disproportionation of 2 equiv of H_2O_2 into 2 equiv of H_2O and 1 equiv of O_2 (Scheme 10; see Supporting Information for details on the simulation). Comparison of Figure 3B and 3A reveals that the rate of isotope scrambling (as measured by incorporation of L^D into **2**) is slower than that predicted if the formation and

DOI: 10.1021/jacs.5b08719
J. Am. Chem. Soc. 2015, 137, 13632–13646

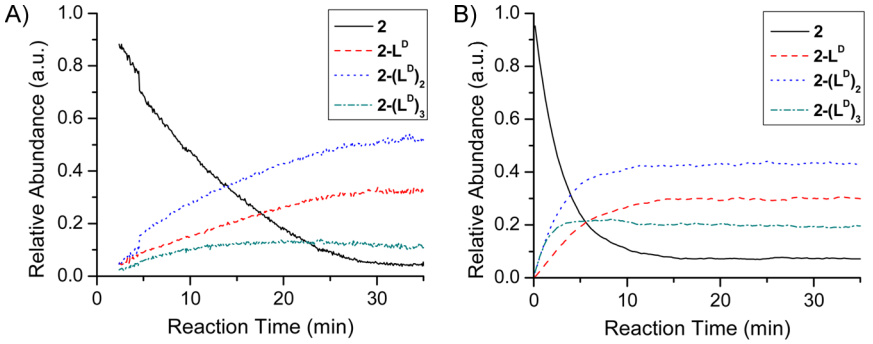

Figure 4. Measured (A) and simulated (B) isotope incorporation into **2** during **PG** oxidation. (A) Relative abundance of **2**, **2**-L^D, **2**-$(L^D)_2$, and **2**-$(L^D)_3$ observed by ESI-MS as a function of reaction time. Conditions: [**2**] = 0.5 mM; [**7**-L^D] + [**7**] = 4.3 mM, **7**-L^D:**7** = 3.3; [**PG**] = 0.3 M in MeCN. (B) Stochastic simulation of the relative abundance of **2**, **2**-L^D, **2**-$(L^D)_2$, and **2**-$(L^D)_3$ as a function of reaction time. The conversion of diol vs time was a constant 1.8 TON/min (mmol of products/mmol of **2**) throughout this experiment.

Scheme 11. Proposed Mechanism for Incorporation of L^D into 2 during PG Oxidation

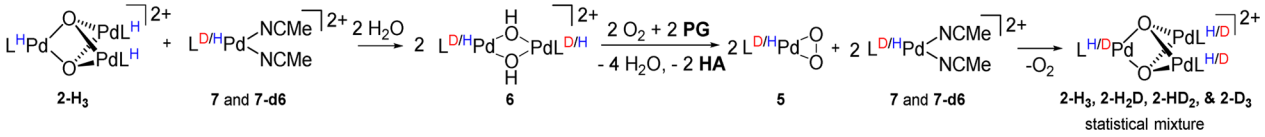

breakup of **2** were to be solely responsible for all of the observed catalysis.[71] These data indicate that **2** is a chemically competent precursor for hydrogen peroxide disproportionation, but that, under the reaction conditions, the trinuclear complex **2** is not the sole reactive intermediate responsible for hydrogen peroxide disproportionation.

The trinuclear $Pd_3O_3^{2+}$ compound $\mathbf{11}^{2+}$ and its L^D isotopologues **11**, **11**-L^D, **11**-$(L^D)_2$, and **11**-$(L^D)_3$ were also observed during this isotope scrambling experiment. The isotopic composition of the detected $\mathbf{11}^{2+}$ reflected the isotopic composition of **7** and **7**-L^D as opposed to the composition of **2**. This fact indicated that **11** is likely formed reversibly in solution from Pd species such as **4** and **6**, as suggested in the isotope labeling and reaction monitoring studies (*vide supra*). These limited data do not provide clear evidence as to whether **11** plays any role in catalysis; however, its presence suggests a rich diversity of multinuclear Pd−O_2 intermediates are present during H_2O_2 disproportionation with **1**.

Role of 2 during Catalysis with 1: Diol Oxidation. As previously reported,[50] the Pd−acetate **1** is an active catalyst for the aerobic oxidation of 1,2-propanediol (propylene glycol, **PG**), and we had previously shown that **2** is formed in the course of alcohol oxidation reactions. Moreover, our previous studies had shown that mixtures of **2** and **7** for the aerobic oxidation of **PG** exhibited similar rates and selectivities as those of the palladium acetate catalyst **1**.[50] To further assess the role of the trinuclear complex **2** in the oxidation of diols, we carried out a similar isotope scrambling experiment where **2** and a mixture of **7** and **7**-L^D were used to catalyze the aerobic oxidation of **PG** to hydroxyacetone (**HA**).

Treatment of a mixture of **2** with **7**-L^D and **7** (**2** = 0.5 mM, [**7**] + [**7**-L^D] = 4.3 mM, **7**-L^D:**7** = 3.3) was used to oxidize **PG** (0.3 M) in MeCN. Conversion to hydroxyacetone was observed by GC analysis of reaction aliquots. Simultaneous online ESI-MS monitoring of this reaction showed that deuterium was incorporated into the population of **2** over 30 min of reaction (Figure 4A; see Scheme 11 for a proposed mechanism). As observed for hydrogen peroxide, the data of Figure 4A clearly indicate that **2** is consumed and regenerated in the course of catalytic alcohol oxidation. Shown in Figure 4B is the predicted speciation of isotopologues of **2** under the assumption that one turnover of **2** would involve the oxidation of 2 equiv of **PG** to **HA** (Scheme 11; see Supporting Information for details on the simulation).[72] This experiment unambiguously illustrates that the rate of deuterium isotope scrambling into **2** is much slower than the oxidation of **PG**. This finding suggests that the formation and breakup of **2** is not the sole mechanism by which reduced Pd species are converted to the active alcohol oxidation catalyst, **1**, or its catalytically active hydroxide analog, **6**.[36]

The results of the isotope scrambling experiments show that, while the formation and conversion of **2** are clearly involved during hydrogen peroxide and alcohol oxidation catalysis, there are multiple simultaneous paths for Pd to reduce oxygen and/or disproportionate H_2O_2 in this system. In the case of O_2 reduction, it is not clear whether O_2 was directly reduced, or if intermediate H_2O_2 is released into solution and subsequently disproportionated.

DFT Predicted Structures of Binuclear $Pd_2O_2^{2+}$. Although we have been able to gather a significant amount of information regarding the chemistry of the trinuclear compound, **2**, there is much less data regarding the transient binuclear complex, **8**. A related species has been proposed as a key intermediate in H_2O_2 disproportionation by tetraaqua Pd^{II} salts.[40] Neutral Pd_2O_2 peroxo compounds are known,[53,73−76] and their chemistry has been investigated. Their activity as oxygen centered bases has been well characterized,[74−78] and some formal O atom transfers have been studied where the O_2 moiety appears to react well with electrophilic reagents, but sluggishly with nucleophilic substrates.[76] Some structural dynamics,[76] equilibria with mononuclear superoxide PdO_2 complexes,[53] and their nucleophilic character have been studied.[76] Given the paucity of studies of dicationic $Pd_2O_2^{2+}$ complexes such as $\mathbf{8}^{2+}$, we conducted a preliminary DFT survey of possible structures for $\mathbf{8}^{2+}$ (Scheme 12), using a level of theory, basis set, and solvent model which has been shown to well predict the chemoselectivity of **1** in oxidizing **PG** (M06l/

DOI: 10.1021/jacs.5b08719
J. Am. Chem. Soc. 2015, 137, 13632−13646

Scheme 12. Calculated Structures for 8^{2+} by DFT

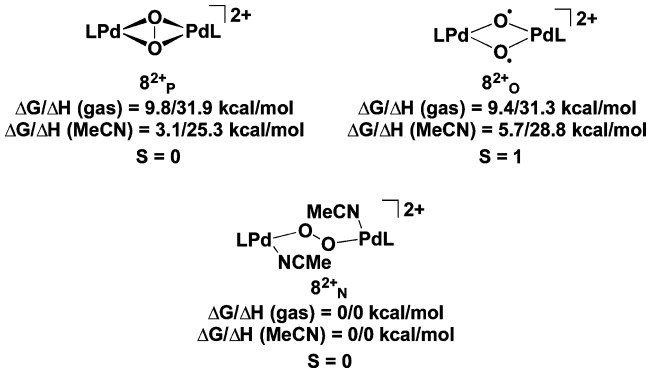

SDDf (Pd)/6-31G(d,p) (HCNO). Solvent model: SMD (MeCN)).[46]

The DFT optimized structure for the μ^2-$\eta^2\eta^2$-peroxo, 8^{2+}_P, was reported previously[50] as a butterfly type structure with an angle of 108° between the planes defined by each PdO_2 unit. The structure also suggests a high degree of strain in each three-membered PdO_2 ring, where the O−Pd−O angle is 38.8°, far from the ideal 90° square planar geometry. The predicted length of the O−O bond of 8^{2+}_P is 1.39 Å. For comparison, the DFT predicted structure of the neutral peroxo **5** has an O−O bond length of 1.39 Å and an O−Pd−O bond angle of 41°, and the reported crystal structure of **5b** has an O−O bond length of 1.41 Å and an O−Pd−O angle of 42°.[26] This suggests that the bond length of the O−O bond in **5** is not significantly affected by coordination to another unit of LPd^{2+}.[79,80] Given the charge of 8^{2+}_P, it is likely that the peroxo is more electrophilic than those of neutral Pd_2O_2 complexes or mononuclear PdO_2 complexes, such as **5**, which tend to react as nucleophiles or bases.[26,34,81−83]

Despite numerous attempts, an optimized structure could not be found for a closed-shell singlet of the μ-oxo compound, 8^{2+}_O, where the O−O bond has been cleaved. Manually increasing the O−O bond length of 8^{2+}_P and minimizing the structure resulted in errors or reoptimizations to 8^{2+}_P. Repeating this process, but as an open shell triplet, resulted in an optimized structure for 8^{2+}_O, which has a planar structure. The distance between the O atoms is 2.48 Å, and the O−Pd−O angles are 78.5°; this bond angle suggests there is a higher degree of bonding between Pd and the oxygen atoms in 8^{2+}_O vs the constrained 8^{2+}_P. Spin density maps indicate that the unpaired electron density lies on each oxygen atom. Thus, the DFT suggests that the O−O bond of 8^{2+}_P can be homolytically cleaved to form 8^{2+}_O, generating two oxyl radical ligands. The calculations suggest that 8^{2+}_P and 8^{2+}_O are essentially isoenergetic, which is surprising given that two oxyl radicals are generated by the reaction. This result is very similar to DFT studies of the conversion of heterobimetallic peroxo complexes of Ni and Zn to a singlet biradical μ-oxo complex, where the spin density was delocalized across the O−Ni−O bonding network.[84] Related investigations of Cu_2O_2 complexes have provided evidence for reversible O−O cleavage of a metal bound peroxo ligand.[79,85−88]

Because these reactions are carried out in acetonitrile as a solvent, we also calculated an additional structure for a bridging peroxo complex, the acetonitrile-coordinated $\mu^{1,2}$-peroxo analog of 8^{2+}_P, 8^{2+}_N. This compound was calculated to be lower in enthalpy by approximately 31.5 kcal/mol than that of the uncoordinated analogs 8^{2+}_P and 8^{2+}_O. These calculations suggest that the mostly likely structure for the bridging peroxo complex **8** in coordinating solvents is that corresponding to 8^{2+}_N; however, ions corresponding to these acetonitrile adducts were not observed in the ESI experiments. It is possible that the acetonitrile was stripped off in the course of the ionization process or the calculations may have overestimated the stability of these adducts.

Comparisons of Hydrogen Peroxide Disproportionation and Alcohol Oxidation with 1. The rates for H_2O_2 disproportionation by Pd−acetate **1** are significantly faster than those for the aerobic oxidation of 1,2-propanediol; H_2O_2 disproportionation varies from 9 to 22 times faster than 1,2-propanediol oxidation under similar conditions (see Supporting Information, Table S12). Thus, assuming the rate law in eq 1 can be extended to low $[H_2O_2]$, if hydrogen peroxide were to be generated during the course of aerobic oxidations with **1**, as commonly proposed,[5,8,20] it would be disproportionated more rapidly than the diols would be oxidized. The current data are not conclusive as to whether free H_2O_2 is released during catalysis, or whether Pd−O_2 intermediates such as **4**, **5**, and **8** react without releasing H_2O_2. In either case, these kinetic results can rationalize why hydrogen peroxide was not observed in the course of aerobic oxidations with **1**.[36] Furthermore, when a H_2O_2 disproportionation is performed in 9:1 MeCN/H_2O at [Pd] = 2.0 mM, $[H_2O_2]$ = 1.0 M, [HOAc] = 10 mM, and in the presence of 1.0 M **PG**, the rate of O_2 production is slightly *accelerated* by a factor of 1.15 relative to the reaction without **PG** (Figure S28). This observation is fully consistent with the hypothesis that H_2O_2 disproportionation occurs concomitantly with diol oxidation.

Monitoring the catalytic disproportionation of hydrogen peroxide by the cationic Pd−acetate **1** by ESI-MS reveals some similarities and differences compared to the case of aerobic diol oxidation by **1**. In the presence of high concentrations of H_2O_2 (H_2O_2 disproportionation experiments), the Pd acetate **1** is consumed rapidly, generating the μ-hydroxy complex **6**, where both oxygens from **6** are derived from H_2O_2. In contrast, for aerobic alcohol oxidations with **1**, both **1** (in its monomeric and dimeric forms) and **6** are observed, and ESI-MS of an aerobic **PG** oxidation using $^{18}O_2$ yields peaks centered about m/z 331.0056 for **6** indicating that the oxygen atoms in 6^{2+} are derived from H_2O during **PG** oxidation.[50] These facts suggest that **6** can equilibrate with **1** during alcohol oxidation when the concentration of H_2O_2 is low; however at higher concentrations of H_2O_2 ($[H_2O_2] \approx 0.1-1.0$ M) the μ-hydroxy complex **6** is consumed faster than it can establish an equilibrium with **1**, HOAc, or H_2O.

A variety of multinuclear Pd oxygen species are observed in both hydrogen peroxide disproportionation and alcohol oxidation. In the ESI-MS studies of the aerobic oxidation of **PG** by **1**, the formation and disappearance of the trinuclear complex 2^{2+} correlated with the rate of **PG** oxidation, but did not correlate with the rate of hydrogen peroxide disproportionation, which is much faster than alcohol oxidation. Ions corresponding to the binuclear Pd μ-oxo **8** were observed during hydrogen peroxide disproportionation, but not during alcohol oxidation. The experiments to date reveal that the formation of **2** from hydrogen peroxide and from alcohols/O_2 provides one pathway for the complete reduction of O_2 to water, but kinetic analysis and isotope labeling experiments reveal that a hydrogen peroxide disproportionation mechanism involving **2** is not the sole or even the primary process; some

DOI: 10.1021/jacs.5b08719
J. Am. Chem. Soc. 2015, 137, 13632−13646

Scheme 13. Proposed Mechanistic Scheme for O_2 Reduction and H_2O_2 Disproportionation during Aerobic PG Oxidation

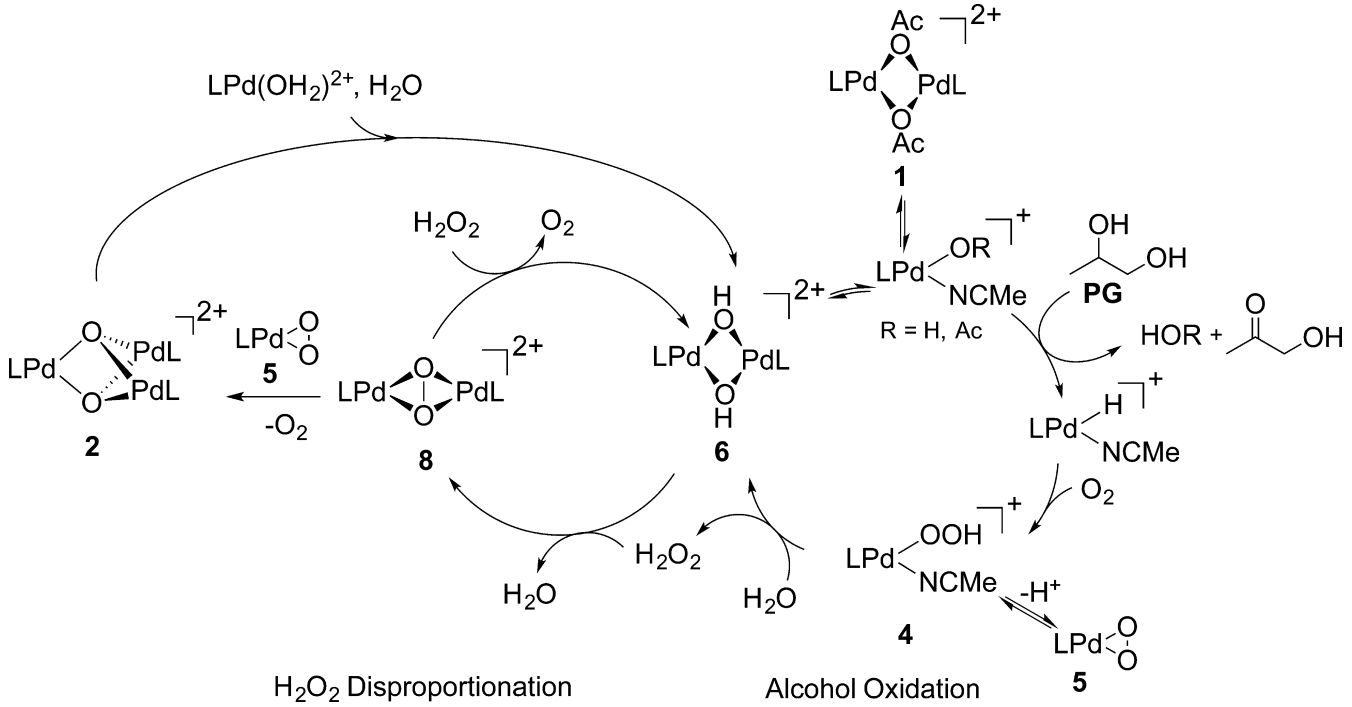

other mechanism must be responsible for the disproportionation of hydrogen peroxide.

The nature of this other process is not yet clear; one proposal is shown in Scheme 13. In this proposal, the dicationic μ-peroxo/oxo **8**, observed by ESI-MS and implicated in the formation of **2**, plays a key branching role, where **8** either reacts with the mononuclear palladium peroxo **5** to form the trinuclear species **2**, as proposed in the synthesis of **2**, or reacts directly with H_2O_2 to produce O_2 and reform the active catalyst **1** and/or **6**. This reactivity would be consistent with the observation that the oxygen atoms of $\mathbf{6}^{2+}$ are derived from H_2O_2. A similar process has been proposed for H_2O_2 disproportionation by tetraaqua Pd^{II} salts[40] and could represent a direct transfer of two hydrogen atoms from H_2O_2 to $\mathbf{8}^{2+}$, as proposed for some synthetic Mn_2O_2-catalase mimics with bis(μ-oxo) cores.[89] That being said, we cannot rule out the involvement of other Pd−O_2 compounds proposed to be intermediates in H_2O_2 disproportionation with other transitions metals (e.g., hydroperoxide, superoxo, peroxo, etc. complexes of Pd) in this process or in the formation of **2**. This is especially true given the known formation of paramagnetic Pd superoxo complexes in mixtures of $Pd_3(OAc)_6$ with H_2O_2.[90−93] In the mechanism proposed in Scheme 13, acetic acid and other protic sources play a key role in converting **2** into the active catalyst **1** or **6**, as determined from the kinetic studies on isolated **2**, and the catalysis and isotope exchange studies utilizing **2** as a precatalyst.

CONCLUSIONS

The stoichiometry of catalytic aerobic alcohol oxidation reactions catalyzed by Pd−acetate compounds necessarily generate partially reduced oxygen species, such as hydrogen peroxide or palladium peroxide complexes. We have shown that aerobic alcohol oxidation reactions with the Pd acetate complex **1** involve the concomitant oxidization of alcohols, activation of O_2, and catalytic disproportionation of hydrogen peroxide by a complicated network of reactions, some of which involve multinuclear Pd−O_2 intermediates. This study is also able to rationalize why H_2O_2 is not observed in the course of the aerobic oxidation of alcohols catalyzed by the Pd−acetate complex **1**. The application of *in situ* electrospray ionization mass spectrometry (ESI-MS), coupled with isotope-labeling and kinetic studies, have provided key insights into several of the reactive intermediates and pathways for alcohol oxidation, oxygen activation, and hydrogen peroxide disproportionation. The results clearly show that, during catalytic aerobic oxidations with the Pd complex **1**, Pd speciates across multiple simultaneous catalytic pathways for oxygen reduction and H_2O_2 disproportionation, one of which involves the trinuclear compound **2** we have previously identified. The presence of such pathways suggests a rich and underexplored chemistry for cationic, multinuclear Pd−O_2 intermediates that are relevant to the reduction of oxygen during aerobic oxidation catalysis with Pd. The detection of $\mathbf{8}^{2+}$ suggests the possibility of electrophilic Pd−O_2 intermediates in solution, which would present an opportunity to explore unique oxygenation chemistry with palladium. Finally, this first mechanistic investigation of hydrogen peroxide disproportionation by the common palladium acetate oxidation catalyst motif exposes a vast and hidden complexity previously unrealized in aerobic oxidation catalysis.

MATERIALS AND METHODS

General. Reagents were purchased from commercial suppliers and used as received apart from 2,6-diisopropylphenol, which was vacuum distilled twice, and H_2O_2, which was titrated with a 0.2 N $KMnO_4$ volumetric standard (Aldrich) to determine molarity. Dry solvents were obtained from an activated alumina column solvent tower (Innovative Technogies PureSolv) and underwent at least two freeze−pump−thaw cycles to degas. Deuterated solvents (Cambridge Isotope Laboratories) were dried over 3 Å molecular sieves, and CD_3CN was stored under a N_2 atmosphere. For manometric kinetics, Optima grade MeCN was used. Deionized water was either Millipore quality or

DOI: 10.1021/jacs.5b08719
J. Am. Chem. Soc. 2015, 137, 13632−13646

obtained directly from the DI water tap; there was no difference detected in the kinetics based on water quality. Solvents for ESI-MS were the highest purity available: Optima grade or as described above from the solvent tower. Air-sensitive compounds were prepared using a Schlenk technique under argon, or inside of a N_2 glovebox where indicated. NMR spectra were recorded on Varian spectrometers at room temperature and referenced to residual protio solvent signals (δ in ppm). $\mathbf{L^D}$,[94] $H_2{}^{18}O_2$,[95,96] **1**,[50] **2**,[50] **5b**,[26] and **7**[50] were synthesized according to literature procedures.

Synthesis of Compounds. *[L^DPd(OAc)]^2(OTf)$_2$ (1-L^D).* **1-$\mathbf{L^D}$** was prepared analogously to literature procedure.[50] $(H_2L^D)(OTf)_2$ was prepared by adding 1 drop of triflic acid to $\mathbf{L^D}$ (20.4 mg, 0.095 mmol) in 0.5 mL of acetone. After 5 min a white powder was precipitated with the addition of 1 mL of diethyl ether, filtered, and washed with additional diethyl ether to yield $(H_2L^D)(OTf)_2$ as a white powder (40.6 mg, 83.3% yield). $\mathbf{L^D}$ (10.1 mg, 0.047 mmol) was dissolved in 0.1 mL of MeCN, and $(H_2L^D)(OTf)_2$ (24.4 mg, 0.047 mmol) was dissolved in 0.1 mL of MeCN. 0.1 mL of MeCN was added to $Pd(OAc)_2$ (21.4 mg, 0.095 mmol); it did not fully dissolve. The $\mathbf{L^D}$ and $(H_2L^D)(OTf)_2$ solutions were added to the $Pd(OAc)_2$, and their vials were rinsed with 0.1 mL of MeCN 5 times. The reaction mixture turned red and homogeneous. After 1 h, 1 mL of diethyl ether was added to precipitate a bright orange powder. It was filtered and washed with additional diethyl ether to yield **1-$\mathbf{L^D}$** as an orange powder (33.0 mg, 66% yield). ^{1}H NMR (500 MHz, d6-DMSO) (monomeric form only with acetic acid added) δ 8.75 (2H, broad d), 8.12 (2H, s), 7.82 (2H, broad d), 3.36 (6H). ^{13}C{H}-NMR (126 MHz, CD_3CN): δ 165.23, 146.61, 139.76, 128.25, 127.70, 126.65, 22.84 (acetate peaks obscured by acetic acid δ 172.10, 21.11). DESI-MS (m/z) in MeCN spray: monomeric $[\mathbf{1\text{-}L^D}]^+$ expected 379.05450, found 379.05313.

[L^DPd(MeCN)$_2$](BF$_4$)$_2$ (7-L^D). **7-$\mathbf{L^D}$** was prepared analogously to **7**.[50] In a glovebox, $\mathbf{L^D}$ (20.0 mg, 0.093 mmol) was dissolved in 1 mL of MeCN and added dropwise with stirring to a 20 mL vial containing a 1 mL MeCN solution of $[Pd(MeCN)_4](BF_4)_2$. The syringe was rinsed two times with 0.9 mL of MeCN each. The pink-yellow reaction mixture was allowed to stir for 1 h before layering with 3.7 mL of diethyl ether, after which a pink powder precipitated. This solution was allowed to sit for 2 days, after which the pink powder had converted into yellow crystalline needles. Another 5 mL of diethyl ether were added, and the solution was allowed to sit for another 4 days. At this point the solution consisted of a floating white suspension above the yellow needles. The white suspension was removed manually with a spatula, and yellow crystals were left in the solution for another 4 days. To isolate the yellow crystals of **7-$\mathbf{L^D}$**, the solution was decanted and the crystals were rinsed 3 times with 3 mL of diethyl ether each and dried under vacuum (37.4 mg, 69.5%). ^{1}H NMR (500 MHz, CD_3CN) δ 8.69 (2H, d, J = 8.4 Hz), 8.04 (2H, s), 7.78 (2H, d, 8.4 Hz), 1.96 (CH_3CN, 6H, s). ^{13}C{H}-NMR (126 MHz, CD_3CN) δ 167.2, 149.2, 142.2, 130.5, 128.5, 128.0.

Spectral data for **2b** (not isolated, see preparation below). ^{1}H NMR (500 MHz, CD_3CN) δ 7.97 (2H, s), 7.77 (2H, s), 7.37 (10H, m), 3.10 (6H, s). ^{13}C{H}-NMR (150 MHz, CD_3CN): δ 165.04, 151.80, 148.18, 136.53, 130.80, 130.55, 130.12, 128.27, 127.76, 125.57, 24.64. ^{19}F NMR (376 MHz, CD_3CN): δ −153.36. ESI-MS (m/z) expected $\mathbf{2b}^{2+}$ 716.09582, found 716.09497.

[(Bathocuproine)Pd(OAc)]$_2$(BF$_4$)$_2$ (1b). Based on an analogous synthesis of $\mathbf{2}(BF_4)_2$.[50] $[(Bathocuproine)H_2](BF_4)_2$ is prepared and isolated as an intermediate compound. In a 20 mL vial, 2.5 mL of acetone were added to bathocuproine (135.5 mg, 0.37 mmol). Not all of bathocuproine dissolved. With vigorous stirring, $[HEt_2O]BF_4$ (0.16 mL, approx 1.12 mmol, 3 equiv) was added dropwise. The solution turned red and became homogeneous. By 5 min, there is significant precipitation of a white solid. After 30 min, the product was precipitated by the addition of 6 mL of diethyl ether, filtered, and washed with further diethyl ether to yield $[(bathocuproine)H_2](BF_4)_2$ as a pale yellow powder (182 mg, 90% yield). ^{1}H NMR 400 MHz CD_3CN: 8.09 (2H, s), 7.99 (2H, s), 7.66 (10H, m), 3.09 (6H, s). To a 50 mL round-bottom flask (RBF), bathocuproine (60.0 mg, 0.17 mmol) and $[bathocuproineH_2]^{2+}(BF_4)_2$ (89.2 mg, 0.17 mmol) were added and dissolved in 5.5 mL of MeCN and 16.8 μL of acetic acid. To this solution $Pd(OAc)_2$ (76.5 mg, 0.34 mmol) was added as a solid, and the walls of the flask were washed with 1 mL of MeCN. The solution was stirred for 6 h, after which the product is precipitated with addition of 40 mL of diethyl ether. Filtration and washing with diethyl ether yielded **1b** as a brown-orange powder (89.5 mg, 44% yield). The product was purified by dissolving it in a minimum volume of 9:1 MeCN/acetic acid and stirring for 20 min, followed by precipitation with ether. Filtration and washing with ether yielded **2b** (40.5 mg, 45% yield). ^{1}H NMR (400 MHz, d6-DMSO) (monomeric form only) δ 7.94 (2H, s), 7.90 (2H, s), 7.66 (10H, m), 2.89 (6H, s), 1.96 (3H, s). ^{13}C{H}-NMR (126 MHz, CD_3CN): δ 178.17, 164.97, 150.69, 147.43, 134.78, 130.06, 129.67, 129.21, 127.55, 126.15, 124.84, 23.97, 22.81. ^{19}F NMR (376 MHz, CD_3CN): δ 148.7. ESI-MS (m/z): monomeric $\mathbf{1b}^+$ expected 525.07997, found 525.08221.

[(Bathocuproine)Pd(MeCN)$_2$](BF$_4$)$_2$ (7b). Inside of a glovebox, $[Pd(MeCN)_4](BF_4)_2$ (222.2 mg, 0.50 mmol) was added to a 50 mL Schlenk flask and dissolved with 10 mL of dry MeCN. To a 20 mL vial, bathocuproine (180.2 mg, 0.50 mmol) and 10 mL of dry MeCN were added. The bathocuproine solution was transferred as a slurry to the Schlenk flask, and residual bathocuproine was washed and transferred with 5 mL of additional MeCN. The resultant red solution was stirred for 3 days until it turned orange-yellow. 28 mL of diethyl ether were added to precipitate the product. This suspension was cannula transferred to a filter and washed two times with 5 mL of diethyl ether. **7b** was dried under vacuum and isolated as a pale yellow powder (285.0 mg, 79% yield). ^{1}H NMR (400 MHz, CD_3CN) δ 7.97 (s, 2H), 7.81 (s, 2H), 7.67 (m, 10H), 3.04 (s, 6H), 1.96 (s, 6H). ^{13}C{H}-NMR (126 MHz, CD_3CN): δ 166.64, 154.12, 149.66, 135.40, 131.45, 130.55, 130.30, 128.76, 128.36, 126.43. ^{19}F-NMR (376 MHz, CD_3CN) δ 152.2. ESI-MS (m/z): $\mathbf{7b}^{2+}$ expected 274.05963, found 274.05966. $[(Bathocuproine)Pd(MeCN)]^{2+}$ expected 253.54633, found 253.54620.

Preparation of Stock Solutions of 2 and 2b. Due to the difficulty in isolating pure samples of **2** and **2b**, stock solutions of **2**(**b**) with varying amounts of residual **7**(**b**) were prepared on demand from the comparatively stable **5**(**b**) and **7**(**b**). The following procedure was used to prepare stock solutions of **2** or **2b**, with modifications made to the procedure for different volumes of stock solution or different desired concentrations. Inside of a glovebox, 1 equiv of **5**(**b**) was added to a vial with a septum cap and a small amount of MeCN was added to make a slurry. **5b** was slightly soluble in MeCN and yielded a cloudy light brown solution while **5** was very insoluble and yielded a very pale yellow supernatant above a brown slurry. Depending on the desired final concentration, 0.5 or more equivalents of **7**(**b**) were dissolved with MeCN in a separate vial to form a yellow solution. The required equivalents of **7**(**b**) were drawn up into a syringe which was then used to puncture the septum cap of the vial containing **5** or **5b** without injecting the solution. The vial and syringe setup was taken out of the glovebox, and the **5** or **5b** solution was sonicated for 30 s before injecting in the **7** or **7b** solution, while still sonicating. The resulting solution was sonicated for an additional 3 min or until the orange solution containing **2**(**b**) with residual **7**(**b**) became clear and homogeneous. Small amounts of oxidized neocuproine biproducts (e.g., **9**(**b**), and **10**(**b**)) were observed in these solutions, and their impact on the chemistry was assumed to be negligible.

Kinetic Studies of Conversion of 1b to 2b. To prepare samples for NMR kinetics experiments, the following general procedure was used. A stock solution of 1.5 mM **2b** and 1.5 mM **7b** was prepared as mentioned above. A 0.3 M benzene stock solution was added as an internal standard such that benzene was 3.1 mM in the **7b** and **7b** solution. 0.7 mL of the solution was added to an NMR tube, and an NMR was taken at the "0" time point. 1.75 μL of glacial acetic acid was added to the NMR tube, and the tube was inverted at least 10 times to initiate the conversion of **2b** to **1b**. NMRs were taken every 5 min, 40 min, or several hours, depending on the time scale of the reaction. When the H_2O, H_2O_2, and pinacol addition experiments were performed, the glacial acetic acid was not added; instead, a stock solution of the additive and acetic acid was added.

Manometric Monitoring of H_2O_2 Disproportionation. H_2O_2 disproportionation kinetics were monitored manometrically with a

DOI: 10.1021/jacs.5b08719
J. Am. Chem. Soc. 2015, 137, 13632−13646

digital pressure transducer connected by USB to a nearby computer (OMEGA Engineering, Stamford, CT). The assembled reactor consisted of the transducer connected by Tygon tubing to a 10 mL Schlenk flask sealed with a rubber septum. The total volume of the reactor was determined by injecting known volumes of air and noting the increase in pressure. The reactor headspace volume was determined by subtracting the volume of the reaction solution. The bulb of the Schlenk flask was entirely submerged in a 25 °C water bath. Discrepancies between the temperature of the headspace and the temperature of the reaction solution are accounted for in the calibration of the total reactor volume. The system was validated by monitoring the rate of H_2O_2 disproportionation by $Fe(ClO_4)_{2(aq)}$ in 1 M $HClO_{4(aq)}$.[97]

To monitor reactions, the following general procedure was used. A solution of H_2O_2 in 11.1% H_2O in MeCN was stirred magnetically for 5−10 min in order to equilibrate the vapor content of the headspace with the solution. Once the pressure reading was constant for at least 1 min, a solution of **2** in 0.1 M HOAc in MeCN was injected by syringe directly into the H_2O_2 solution. For most every reaction, the H_2O_2 solution contributed 90% of the total reaction volume, and the solution of **2** contributed 10%. After injection, a calibrated amount of headspace volume was removed such that the vapor pressures were already at equilibrium with the reaction solution. The amount of removed headspace volume was calibrated by injecting blank solutions (0.1 M HOAc in MeCN) into equilibrated H_2O_2 solutions and removing different amounts of headspace until the resulting pressure vs time curve was flat. This way, any pressure increase could be attributed to the production of $O_{2(g)}$. The solubility of O_2 in MeCN is approximately 13 mM/torr O_2,[98,99] which corresponded to less than 5% of the produced $O_{2(g)}$. Therefore, dissolved oxygen was generally neglected during data analysis. Control experiments were performed to ensure that gas diffusion from solution into the headspace was not rate limiting. Specifically, different total reaction volumes that gave very different rates of P_{O_2} increase yielded identical rate constants, and the stir rate did not affect the measured rate constants.

Mass Spectrometry Details. Depending on resolution requirements, mass spectrometry experiments were conducted either on an LTQ-Orbitrap XL instrument, capable of resolutions up to 100 000 at m/z 400, or an Orbitrap Fusion mass spectrometer, capable of resolutions up to 450 000 at m/z 400. Both were manufactured by Thermo Fisher Scientific (San Jose, CA). For compound identification and ^{18}O-labeling experiments, the high resolution of the Orbitrap Fusion instrument was required to resolve $\mathbf{6}^{2+}$ from $\mathbf{8}^{2+}$ and the various intercalated isotopologues of each compound. In these experiments, aqueous solutions of H_2O_2 were added to 0.1 mM solutions of **1** in MeCN. The resulting reaction solutions were drawn into gastight syringes and infused directly into the HESI ion source of the instrument. Data were preliminarily analyzed in the Thermo Fisher's Qual Browser tool and then exported as text files for further processing in MatLab. Assignments made were within 5 ppm mass accuracy for >96% of assigned peaks, which is the expected accuracy and precision for the resolution of the instrument. At a resolution of 450 000, there are generally multiple, partially overlapping isotopologues at each nominally isobaric mass for the Pd-containing compounds. This complexity was such that simple peak heights and areas were not used to fit the data. Instead, direct sums of simulated spectra were used to fit spectra for each compound and determine isotopic distributions at this resolution (see Supporting Information for details).

Online reaction monitoring and isotope labeling experiments using deuterium mass labels were performed on a hybrid LTQ-Orbitrap XL instrument (Thermo Fisher Scientific, San Jose, CA), capable of resolutions up to 100 000 at m/z 400. Online reaction monitoring experiments were conducted using McIndoe's pressurized infusion method,[62−64] which consists of running a reaction in a standard septum sealed Schlenk flask overpressurized with 1−7 psi N_2. The end of a length of PEEK tubing was fed through the septum and placed below the level of the solution such that the over pressure on the flask forces solution through the tubing at flow rates between 2 and 20 μL/min. The flow rate is controlled by adjusting the overpressure of the flask. The other end of the tubing can be connected directly to the ESI ion source, or if required, online dilutions of up to 20-fold can be achieved by connecting this tubing to a mixing-T that leads to the ESI ion source and supplying a flow of diluent with an external syringe pump. The custom ESI ion source used in these experiments has been described previously.[50]

A reaction between **1** and H_2O_2 was monitored by stirring 5.4 mL of a 1 M H_2O_2 solution in 11.1% H_2O in MeCN in a 10 mL Schlenk flask pressurized to 5 psi with $N_{2(g)}$. A piece of 89 μm ID PEEK tubing was used to transfer this solution to a mixing-T, where it was diluted by a 0.1 mL/min flow of 10% H_2O in MeCN before traveling to a custom ESI source placed in front of the inlet of the instrument. Careful adjustment of overpressure and diluent flow rate is required for a steady signal. 0.6 mL of 0.01 M **1** in 0.1 M HOAc in MeCN was added by syringe to initiate the reaction. It took approximately 1 min for Pd containing peaks to appear in the mass spectrum, corresponding to the amount of time the solution travels in the PEEK tubing before reaching the ion source. The production of O_2 was monitored in a simultaneous, parallel experiment.

Isotope Scrambling Experiment. The isotope scrambling experiments with **2** were conducted similarly to the monitoring experiments of the reactions between **1** and H_2O_2 (*vide supra*). For the isotope scrambling experiment monitoring **PG** oxidation, 2 mL of a solution of 0.5 mM **2**-$(\mathbf{L^H})_3$, 1.0 mM **7**, and 3.33 mM **7**-$\mathbf{L^D}$ were stirred in a septum-sealed 10 mL Schlenk flask pressurized to approximately 4 psi with compressed air. A piece of 89 μm ID PEEK tubing was used to transfer this solution to a mixing-T, where it was diluted by a 0.1 mL/min flow of MeCN before traveling to a custom ESI source placed in front of the inlet of the instrument. 44 mL (46 mg, 0.60 mmol) of neat **PG** were added by microsyringe, and the exchange of **2**-$(\mathbf{L^H})_3$ for a statistical mixture of isotopically labeled compounds was monitored for 30 min. Approximately 50 μL aliquots of this reaction were taken every 2−3 min and passed immediately through silica plugs with an additional 3−4 mL of MeCN to quench the reaction for GC analysis. Production of **HA** was determined using the calibrated relative sensitivities of **HA** and **PG** assuming that the [**PG**] + [**HA**] was constant. The isotope scrambling experiment with H_2O_2 was performed by stirring 0.9 mL of a 1.11 M solution of H_2O_2 in 11.1% H_2O in MeCN in a septum-sealed 10 mL Schlenk flask pressurized to 6 psi and interfaced with the MS instrument as mentioned above. 0.1 mL of a solution of 1.1 mM **2**-$(\mathbf{L^H})_3$, 1.3 mM **7**, and 5 mM **7**-$\mathbf{L^D}$ was added by syringe such that the final concentrations were as follows: $[H_2O_2]$ = 1.0 M, [**2**-$(\mathbf{L^H})_3$] = 0.11 mM, [**7**] = 0.13 mM, [**7**-$\mathbf{L^D}$] = 0.5 mM. ESI-MS data were gathered for 15 min; however, exchange was complete within 8 min. An independent reaction was monitored manometrically (as mentioned above) using 5.4 mL of the H_2O_2 stock solution and 0.6 mL of the Pd stock solution.

■ ASSOCIATED CONTENT

Supporting Information

The Supporting Information is available free of charge on the ACS Publications website at DOI: 10.1021/jacs.5b08719.

Synthetic procedures, NMR and mass spectra, mechanistic experiments (PDF)

■ AUTHOR INFORMATION

Corresponding Author

*waymouth@stanford.edu

Notes

The authors declare no competing financial interest.

■ ACKNOWLEDGMENTS

A.J.I. is grateful for a Robert M. Bass and Anne T. Bass Stanford Graduate Fellowship, a National Science Foundation Graduate Research Fellowship, and a Center for Molecular Analysis and

Design Graduate Fellowship. R.N.Z. gratefully acknowledges financial support from a subcontract with the University of Utah (Agreement No. 10029173-S2) for which the Air Force Office of Scientific Research (Grant FA9550-12-1-0481) is the prime sponsor. R.M.W. acknowledges support from the Department of Energy (DE-SC0005430).

REFERENCES

(1) Punniyamurthy, T.; Velusamy, S.; Iqbal, J. *Chem. Rev.* **2005**, *105*, 2329.
(2) Shi, Z.; Zhang, C.; Tang, C.; Jiao, N. *Chem. Soc. Rev.* **2012**, *41*, 3381.
(3) Que, L.; Tolman, W. B. *Nature* **2008**, *455*, 333.
(4) Boisvert, L.; Goldberg, K. I. *Acc. Chem. Res.* **2012**, *45*, 899.
(5) Stahl, S. S. *Angew. Chem., Int. Ed.* **2004**, *43*, 3400.
(6) Gligorich, K. M.; Sigman, M. S. *Chem. Commun.* **2009**, 3854.
(7) Stahl, S. S. *Science* **2005**, *309*, 1824.
(8) Gligorich, K. M.; Sigman, M. S. *Angew. Chem., Int. Ed.* **2006**, *45*, 6612.
(9) Cornell, C. N.; Sigman, M. S. *Inorg. Chem.* **2007**, *46*, 1903.
(10) Sigman, M. S.; Jensen, D. R. *Acc. Chem. Res.* **2006**, *39*, 221.
(11) Schultz, M. J.; Sigman, M. S. *Tetrahedron* **2006**, *62*, 8227.
(12) Sheldon, R. A.; Arends, I. W. C. E.; ten Brink, G.-J.; Dijksman, A. *Acc. Chem. Res.* **2002**, *35*, 774.
(13) Wu, W.; Jiang, H. *Acc. Chem. Res.* **2012**, *45*, 1736.
(14) McDonald, R. I.; Liu, G.; Stahl, S. S. *Chem. Rev.* **2011**, *111*, 2981.
(15) Beccalli, E. M.; Broggini, G.; Martinelli, M.; Sottocornola, S. *Chem. Rev.* **2007**, *107*, 5318.
(16) Yeung, C. S.; Dong, V. M. *Chem. Rev.* **2011**, *111*, 1215.
(17) Lyons, T. W.; Sanford, M. S. *Chem. Rev.* **2010**, *110*, 1147.
(18) Chen, X.; Engle, K. M.; Wang, D. H.; Yu, J. Q. *Angew. Chem., Int. Ed.* **2009**, *48*, 5094.
(19) Izawa, Y.; Pun, D.; Stahl, S. S. *Science* **2011**, *333*, 209.
(20) Muzart, J. *Chem. - Asian J.* **2006**, *1*, 508.
(21) Denney, M. C.; Smythe, N. A.; Cetto, K. L.; Kemp, R. A.; Goldberg, K. I. *J. Am. Chem. Soc.* **2006**, *128*, 2508.
(22) Cai, X.; Majumdar, S.; Fortman, G. C.; Cazin, C. S.; Slawin, A. M.; Lhermitte, C.; Prabhakar, R.; Germain, M. E.; Palluccio, T.; Nolan, S. P.; Rybak-Akimova, E. V.; Temprado, M.; Captain, B.; Hoff, C. D. *J. Am. Chem. Soc.* **2011**, *133*, 1290.
(23) Popp, B. V.; Stahl, S. S. *J. Am. Chem. Soc.* **2006**, *128*, 2804.
(24) Popp, B. V.; Stahl, S. S. *Chem. - Eur. J.* **2009**, *15*, 2915.
(25) Landis, C. R.; Morales, C. M.; Stahl, S. S. *J. Am. Chem. Soc.* **2004**, *126*, 16302.
(26) Stahl, S. S.; Thorman, J. L.; Nelson, R. C.; Kozee, M. A. *J. Am. Chem. Soc.* **2001**, *123*, 7188.
(27) Steinhoff, B. A.; Guzei, I. A.; Stahl, S. S. *J. Am. Chem. Soc.* **2004**, *126*, 11268.
(28) Valentine, J. S. *Chem. Rev.* **1973**, *73*, 235.
(29) Steinhoff, B. A.; Stahl, S. S. *Org. Lett.* **2002**, *4*, 4179.
(30) Keith, J. M.; Nielsen, R. J.; Oxgaard, J.; Goddard, W. A. *J. Am. Chem. Soc.* **2005**, *127*, 13172.
(31) Decharin, N.; Popp, B. V.; Stahl, S. S. *J. Am. Chem. Soc.* **2011**, *133*, 13268.
(32) Chowdhury, S.; Rivalta, I.; Russo, N.; Sicilia, E. *Chem. Phys. Lett.* **2007**, *443*, 183.
(33) Chowdhury, S.; Rivalta, I.; Russo, N.; Sicilia, E. *Chem. Phys. Lett.* **2008**, *456*, 41.
(34) Konnick, M. M.; Gandhi, B. A.; Guzei, I. A.; Stahl, S. S. *Angew. Chem., Int. Ed.* **2006**, *45*, 2904.
(35) Konnick, M. M.; Guzei, I. A.; Stahl, S. S. *J. Am. Chem. Soc.* **2004**, *126*, 10212.
(36) Conley, N. R.; Labios, L. A.; Pearson, D. M.; McCrory, C. C. L.; Waymouth, R. M. *Organometallics* **2007**, *26*, 5447.
(37) Strukul, G.; Ros, R.; Michelin, R. A. *Inorg. Chem.* **1982**, *21*, 495.
(38) Bianchi, D.; Bortolo, R.; D'Aloisio, R.; Ricci, M. *Angew. Chem., Int. Ed.* **1999**, *38*, 706.
(39) Steinhoff, B. A.; Fix, S. R.; Stahl, S. S. *J. Am. Chem. Soc.* **2002**, *124*, 766.
(40) Potekhin, V. V.; Solov'eva, S. N.; Potekhin, V. M. *Russ. Chem. Bull.* **2005**, *54*, 1105.
(41) Grinberg, A. A.; Kukushkin, Y. N.; Vlasova, R. A. *Zh. Neorg. Khim.* **1968**, *13*, 2177.
(42) Kukushkin, Y. N.; Vlasova, R. A. *J. Appl. Chem.-USSR.* **1968**, *41*, 1407.
(43) Lomova, T. N.; Klyueva, M. E.; Kosareva, O. V.; Klyuev, M. V. *Russ. J. Phys. Chem. A* **2008**, *82*, 1086.
(44) Pearson, D. M.; Conley, N. R.; Waymouth, R. M. *Organometallics* **2011**, *30*, 1445.
(45) Painter, R. M.; Pearson, D. M.; Waymouth, R. M. *Angew. Chem., Int. Ed.* **2010**, *49*, 9456.
(46) Chung, K.; Banik, S. M.; De Crisci, A. G.; Pearson, D. M.; Blake, T. R.; Olsson, J. V.; Ingram, A. J.; Zare, R. N.; Waymouth, R. M. *J. Am. Chem. Soc.* **2013**, *135*, 7593.
(47) De Crisci, A. G.; Chung, K.; Oliver, A. G.; Solis-Ibarra, D.; Waymouth, R. M. *Organometallics* **2013**, *32*, 2257.
(48) Blake, T. R.; Waymouth, R. M. *J. Am. Chem. Soc.* **2014**, *136*, 9252.
(49) Jäger, M.; Hartmann, M.; de Vries, J. G.; Minnaard, A. J. *Angew. Chem., Int. Ed.* **2013**, *52*, 7809.
(50) Ingram, A. J.; Solis-Ibarra, D.; Zare, R. N.; Waymouth, R. M. *Angew. Chem., Int. Ed.* **2014**, *53*, 5648.
(51) Aboelella, N. W.; York, J. T.; Reynolds, A. M.; Fujita, K.; Kinsinger, C. R.; Cramer, C. J.; Riordan, C. G.; Tolman, W. B. *Chem. Commun.* **2004**, 1716.
(52) York, J. T.; Llobet, A.; Cramer, C. J.; Tolman, W. B. *J. Am. Chem. Soc.* **2007**, *129*, 7990.
(53) Huacuja, R.; Graham, D. J.; Fafard, C. M.; Chen, C.-H.; Foxman, B. M.; Herbert, D. E.; Alliger, G.; Thomas, C. M.; Ozerov, O. V. *J. Am. Chem. Soc.* **2011**, *133*, 3820.
(54) The ^{1}H NMR signals for **9** were initially assigned to a Pd–methanolate complex (see Conley et al. ref 36) and have been reassigned to the peroxide **9**. In the course of this work, the Pd–methanolate complex was not observed in ESI-MS of reaction mixtures and is likely only formed in trace amounts.
(55) See Supporting Information for details.
(56) Converison of **1** to **9** requires 2 equiv of H_2O_2 (i.e., 1 equiv of O_2). Conversion of **1** to **3** or **10** requires 3 equiv of H_2O_2 (i.e., 1.5 equiv of O_2).
(57) See the Material and Methods section as well as Supporting Information for details regarding the kinetics experiments. Proper control experiments and calibrations were performed to ensure that the pressure increase corresponded directly to PO_2.
(58) Catalytic performance of stock solutions of **1** prepared without HOAc were not stable, due to the precipitation of the less soluble **6**, formed from the reaction of **1** with trace H_2O.
(59) We cannot conclusively rule out reversible binding of the Pd catalyst as a explanation for the decreased activity; however, BHT and DiPP have nearly identical impacts on the rate of O_2 production while their sterics are very different. Their similar activity indicates that binding the active catalyst as a phenolate complex is not the principal reason for the decrease in H_2O_2 disproportion rates.
(60) Ogata, M.; Tutumimoto Sato, K.; Kunikane, T.; Oka, K.; Seki, M.; Urano, S.; Hiramatsu, K.; Endo, T. *Biol. Pharm. Bull.* **2005**, *28*, 1120.
(61) Ryan, D. A.; Espenson, J. H. *J. Am. Chem. Soc.* **1982**, *104*, 704.
(62) Vikse, K. L.; Ahmadi, Z.; Luo, J.; van der Wal, N.; Daze, K.; Taylor, N.; McIndoe, J. S. *Int. J. Mass Spectrom.* **2012**, *323-324*, 8.
(63) Vikse, K. L.; Ahmadi, Z.; Manning, C. C.; Harrington, D. A.; McIndoe, J. S. *Angew. Chem., Int. Ed.* **2011**, *50*, 8304.
(64) Vikse, K. L.; Woods, M. P.; McIndoe, J. S. *Organometallics* **2010**, *29*, 6615.
(65) Senko, M. W.; Remes, P. M.; Canterbury, J. D.; Mathur, R.; Song, Q.; Eliuk, S. M.; Mullen, C.; Earley, L.; Hardman, M.; Blethrow, J. D.; Bui, H.; Specht, A.; Lange, O.; Denisov, E.; Makarov, A.; Horning, S.; Zabrouskov, V. *Anal. Chem.* **2013**, *85*, 11710.

DOI: 10.1021/jacs.5b08719
J. Am. Chem. Soc. 2015, 137, 13632–13646

(66) Zubarev, R. A.; Makarov, A. *Anal. Chem.* **2013**, *85*, 5288.
(67) Experiments involving $H_2{}^{18}O_2$ were performed under a N_2 atmosphere. Under air, signficant amounts of $^{16}O_2$ scrambled into the solution by an unknown mechanism.
(68) Rush, J. D.; Maskos, Z. *Inorg. Chem.* **1990**, *29*, 897.
(69) Santos, L. S. *Eur. J. Org. Chem.* **2008**, *2008*, 235.
(70) No ligand subsitution was observed within minutes at room temperature in a mixture of **5b** and neocuproine. The formation of **2** is fast and occurs in under 1 min at room temperature; therefore, direct exchange of L^D for L^H at **5** is not a reasonable explanation for the observed scrambling process.
(71) Close inspection of Figure 4 shows higher deuterium incorporation into **2** than expected. This is likely due to a kinetic isotope effect for the decomposition of the catalyst which enriches the deuterium label at later reaction times. This kinetic isotope effect on catalyst stability has been reported for **1**-L^D, the deuterated form of **1**.
(72) If [**2**] during catalysis is lower than the initial $[\mathbf{2}]_0$, which is expected, then the measured rate of isotope incorporation should be faster than the simulated incorporation. Since, as the population of **2** is diminished, the relative abundance of **2**-$(L^D)_1$, **2**-$(L^D)_2$, and **2**-$(L^D)_3$ produced by catalysis is increased relative to the observed ions corresponding to **2**.
(73) Suzuki, H.; Mizutani, K.; Morooka, Y.; Ikawa, T. *J. Am. Chem. Soc.* **1979**, *101*, 748.
(74) Chung, P. J.; Suzuki, H.; Moro-Oka, Y.; Ikawa, T. *Chem. Lett.* **1980**, 63.
(75) Akita, M.; Miyaji, T.; Moro-oka, Y. *Chem. Commun.* **1998**, 1005.
(76) Miyaji, T.; Kujime, M.; Hikichi, S.; Moro-oka, Y.; Akita, M. *Inorg. Chem.* **2002**, *41*, 5286.
(77) Sugimoto, R.; Eikawa, H.; Suzuki, H.; Moro-oka, Y.; Ikawa, T. *Bull. Chem. Soc. Jpn.* **1981**, *54*, 2849.
(78) Chung, P. J. *J. Korean Chem. Soc.* **1986**, *30*, 516.
(79) Solomon, E. I.; Ginsbach, J. W.; Heppner, D. E.; Kieber-Emmons, M. T.; Kjaergaard, C. H.; Smeets, P. J.; Tian, L.; Woertink, J. S. *Faraday Discuss.* **2011**, *148*, 11.
(80) Solomon, E. I.; Sundaram, U. M.; Machonkin, T. E. *Chem. Rev.* **1996**, *96*, 2563.
(81) Maeda, K.; Moritani, I.; Hosokawa, T.; Murahashi, S.-I. *Tetrahedron Lett.* **1974**, *15*, 797.
(82) Bellon, P. L.; Cenini, S.; Demartin, F.; Manassero, M.; Pizzotti, M.; Porta, F. *J. Chem. Soc., Dalton Trans.* **1980**, 2060.
(83) Yamashita, M.; Goto, K.; Kawashima, T. *J. Am. Chem. Soc.* **2005**, *127*, 7294.
(84) Yao, S.; Xiong, Y.; Vogt, M.; Grützmacher, H.; Herwig, C.; Limberg, C.; Driess, M. *Angew. Chem., Int. Ed.* **2009**, *48*, 8107.
(85) Halfen, J. A.; Mahapatra, S.; Wilkinson, E. C.; Kaderli, S.; Young, V. G.; Que, L.; Zuberbuhler, A. D.; Tolman, W. B. *Science* **1996**, *271*, 1397.
(86) Hatcher, L. Q.; Vance, M. A.; Narducci Sarjeant, A. A.; Solomon, E. I.; Karlin, K. D. *Inorg. Chem.* **2006**, *45*, 3004.
(87) Mahapatra, S.; Kaderli, S.; Llobet, A.; Neuhold, Y.-M.; Palanché, T.; Halfen, J. A.; Young, V. G.; Kaden, T. A.; Que, L.; Zuberbühler, A. D.; Tolman, W. B. *Inorg. Chem.* **1997**, *36*, 6343.
(88) Ottenwaelder, X.; Rudd, D. J.; Corbett, M. C.; Hodgson, K. O.; Hedman, B.; Stack, T. D. P. *J. Am. Chem. Soc.* **2006**, *128*, 9268.
(89) Larson, E. J.; Pecoraro, V. L. *J. Am. Chem. Soc.* **1991**, *113*, 7809.
(90) Talsi, E. P.; Babenko, V. P.; Chinakov, V. D.; Nekipelov, V. M. *React. Kinet. Catal. Lett.* **1986**, *32*, 347.
(91) Talsi, E. P.; Babenko, V. P.; Likholobov, V. A.; Nekipelov, V. M.; Chinakov, V. D. *J. Chem. Soc., Chem. Commun.* **1985**, 1768.
(92) Talsi, E. P.; Babenko, V. P.; Nekipelov, V. M.; Shubin, A. A. *React. Kinet. Catal. Lett.* **1986**, *31*, 209.
(93) Talsi, E. P.; Babenko, V. P.; Shubin, A. A.; Chinakov, V. D.; Nekipelov, V. M.; Zamaraev, K. I. *Inorg. Chem.* **1987**, *26*, 3871.
(94) Pijper, P. J.; van der Goot, H.; Timmerman, H.; Nauta, W. T. *Eur. J. Med. Chem.* **1984**, *19*, 399.
(95) Jankowski, S.; Kamiński, R. *J. Labelled Compd. Radiopharm.* **1995**, *36*, 373.
(96) Sitter, A. J.; Terner, J. *J. Labelled Compd. Radiopharm.* **1985**, *22*, 461.
(97) Voloshin, Y.; Manganaro, J.; Lawal, A. *Ind. Eng. Chem. Res.* **2008**, *47*, 8119.
(98) Horstmann, S.; Grybat, A.; Kato, R. *J. Chem. Thermodyn.* **2004**, *36*, 1015.
(99) Franco, C.; Olmsted Iii, J. *Talanta* **1990**, *37*, 905.

DOI: 10.1021/jacs.5b08719
J. Am. Chem. Soc. 2015, 137, 13632−13646